High-intensity neutron spectroscopy of nuclei

L. B. Pikel'ner, Yu. P. Popov, and É. I. Sharapov

Joint Institute for Nuclear Research, Dubna (Moscow District)

The use of neutron spectroscopy to study the properties of nuclei is reviewed. The development of neutron spectroscopy over the years and the principal results are discussed briefly. The experimental methods of neutron spectroscopy are described. Emphasis is placed on the new directions in neutron spectroscopy of nuclei: the alpha decay of compound states excited during neutron capture by nuclei, hyperfine interactions in neutron resonances, and the properties of few-nucleon nuclei in reactions with neutrons. The most important experimental results are discussed and compared with the theory.

PACS numbers: 29.30.Hs

CONTENTS

1. INTRODUCTION

Chadwick's discovery of the neutron[1] in 1932 sparked a genuine revolution in our understanding of nuclear structure. The proton–electron model of the nucleus was deposed by the proton–neutron model of Ivanenko (Iwanenko[2]) and Heisenberg,[3] which furnished an explanation of reinterpretation of several established facts. This new model was to have a major effect on the course of subsequent research.

Soon after the discovery of the neutron, Fermi reported his first experiments on nuclear reactions induced by neutrons.[4] Only four years after the discovery of the neutron, Fermi's group, and also Moon and Tillman,[5] observed individual neutron resonances. In an effort to explain the existence and properties of these narrow, highly excited states, Niels Bohr advanced the hypothesis of a compound nucleus.[6] The decade ended with Hahn and Strassmann's discovery of neutron-induced nuclear fission[7] and Zel'dovich and Khariton's derivation of a theory for the chain reaction.[8]

These events had a tremendous influence on nuclear science and perhaps on modern civilization in general.

Quite rapidly, fundamental experimental and theoretical research led to the development of neutron physics as a highly important branch of nuclear physics and laid the scientific basis for modern nuclear power. Over the same years, neutron spectroscopy of nuclei arose as a branch of neutron physics. Niels Bohr's hypothesis of the compound nucleus and the extensive data which neutron spectroscopy subsequently yielded laid the basis for the statistical theory of the nucleus (Bethe and Weisskopf, 1937–1940) and the R-matrix theory of nuclear reactions (Wigner and Eisenbud, 1948). These theories initially had no competition in describing the mechanisms for neutron–nucleus interactions, but eventually they had to make room for the optical model (Feshbach, Porter, and Weisskopf, 1954). Neutron physics also made an important contribution to the development of our understanding of the nuclear forces acting between nucleons. Study of the np and nd interactions and of the properties of the simplest few-nucleon systems (Feenberg, Wigner, and Schwinger, 1935–1941) led to the hypothesis of the charge independence of nuclear forces. This hypothesis became one of the foundations of the theory for the lightest nuclei.

Throughout all these developments in neutron physics, the primary source of experimental data was neutron spectroscopy. Contemporary research in nuclear physics by neutron methods is so extensive and so rich in results that the subject cannot be covered in a single paper, and we will have to omit many interesting questions from this review. A detailed review of the emergence of neutron physics as a science has been written by an active participant in that development, E. Amaldi.[9] We have not cited all the early papers here, since they are cited in the extensive bibliography furnished by Amaldi. Reviews or monographs have also been published on the physics of fast neutrons,[10] on the γ spectroscopy of the radiative capture of neutrons,[11] and on parity nonconservation in neutron reactions.[12] Nuclear fission induced by neutrons is covered in the journals and conference proceedings (see Ref. 13, for example).

The present review is intended to describe the progress in the use of neutrons to study the properties of compound nuclear states and few-nucleon systems, primarily in the nontraditional directions which arose over the past 10–15 years as a result of the development of several new experimental methods, primarily high-intensity neutron spectrometry. To some extent, the choice of topics has been determined by our own interests and our own fields of study. For an introduction to the present state of other branches of neutron spectroscopy of nuclei we recommend the comprehensive paper by Chrien[14] on nuclear reactions involving resonance neutrons.

2. STUDY OF EXCITED NUCLEAR STATES BY NEUTRON SPECTROMETRY

Since the neutron does not have an electric charge, so that no Coulomb barrier opposes its penetration into a nucleus, it has been possible to use the neutron as a universal tool for exciting essentially all nuclei in the β-stability valley. The methods of neutron spectroscopy have made it possible to study excited compound states of nuclei near the neutron binding energy ($B_n \approx 7$–10 MeV). The procedure here is to analyze the cross sections for the interactions of neutrons with the nucleus. The effective neutron cross section σ_t is a measure of the interaction probability, given by

$$dN = N\sigma_t dn, \tag{1}$$

where dN is the number of neutrons which have interacted in a layer dn (nuclei per square centimeter) of the matter, and N is the number of neutrons incident on this layer.

Compound nuclear states are not stationary states. Their lifetime τ is about 10^{-15} s, and their energy width, determined by the Heisenberg relation $\Gamma = \hbar/\tau$, is 0.66 eV for $\tau = 10^{-15}$ s.

If the nuclear reaction is treated as a process which occurs in two independent steps, the reaction cross section can be written

$$\sigma_x = \sigma_c w(x), \tag{2}$$

where σ_c is the cross section for the production of the compound nucleus, and $w(x) = \Gamma_x/\Gamma$ is the relative
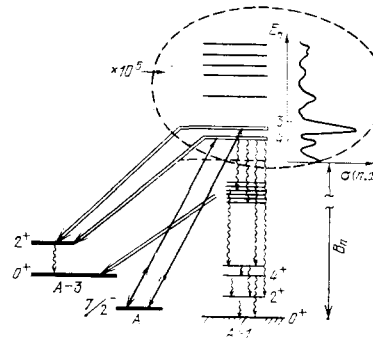

FIG. 1. Excited nuclear levels studied by neutron spectroscopy.

probability for decay through the emission of the particle x. The energies and widths of nuclear levels can be determined by studying the resonances in the dependence of the cross sections on the neutron energy. By detecting the emission of the various particles which are reaction products, it is possible to draw conclusions regarding the partial probabilities for the decay of the compound nuclei (in other words, of the neutron resonances) through various channels. The diagram in Fig. 1 shows the various channels for the decay of neutron resonances and the relationship between the cross sections and the positions of the excited nuclear states. In this example, the capture of an s-wave neutron by the target nucleus A ($I^{\pi} = 7/2^{-}$) gives rise to the excitation in the $(A+1)$ nucleus of compound states with spins $J^{\pi} = 3^{-}, 4^{-}$, above the neutron binding energy B_n. These levels may decay through the emission of a neutron (the inverse process), through the emission of γ rays (the wavy lines), and through the emission of α particles (double lines with arrows). For each process there is a corresponding cross section σ_x.

a) Breit-Wigner parametrization of the cross section

The total neutron cross section σ_t is the sum

$$\sigma_t = \sigma_s + \sigma_\gamma + \sigma_f + \sigma_\alpha + \sigma_p \ldots \tag{3}$$

of the partial cross sections corresponding to scattering, capture, fission, and reactions involving the emission of α particles, protons, etc.

For most nuclei the cross sections σ_s and σ_γ are predominant in this sum at resonance energies. The cross sections σ_p are characteristic of light nuclei, and the fission cross sections σ_f are characteristic of heavy nuclei. The cross sections σ_α are usually small but are known for many nuclei (Sec. 3). The most rigorous description of the energy dependence of the effective cross sections is given by the R-matrix theory, which is set forth in Ref. 15, among other places. The single-level approximation of this theory leads to the well-known formula derived by Breit and Wigner[16]:

$$\sigma_x = \pi \lambda_0^2 g_J \frac{\Gamma_n(E_0)\Gamma_x}{(E-E_0)^2 + (\Gamma^2/4)} ; \tag{4}$$

here E_0 is the resonance energy, λ_0 is the neutron wavelength at $E = E_0$, divided by 2π, $\Gamma_n(E_0)$ is the neu-

tron width at $E = E_0$, Γ_x is the width of the corresponding reaction, and $\Gamma = \Sigma\Gamma_i$ is the total width of the level.

The shape of the resonance is significantly affected by the chemical binding and by the thermal motion of the atoms in a sample (Sec. 4). Furthermore, the shape of the resonance in the reaction cross section is not symmetric because of the factor $\lambda \sim 1/v$, which gives rise to the "$1/v$ law" in the limit $E \to 0$, which is well known in the absorption of slow neutrons.

A statistical weight $g_J = (2J+1)/(2I+1) \times (2s+1)$ arises when the spins I and s of the particles involved in the reaction are combined with their relative orbital angular momentum L to form the total spin of the resonance, $J = L + s + I$. For neutrons with energies below 100 keV, the interaction is dominated by two partial waves, $l = 0$ ("s neutrons") and $l = 1$ ("p neutrons").

In addition to their spin J, the resonances are characterized by one more quantum number: their parity. The parities of the resonances are the same as (opposite to) that of the ground state of the target nucleus if the nucleus is excited by s neutrons (p neutrons).

According to Bohr's concept of the compound nucleus, the neutron resonance is a long-lived nuclear state which decays by a mechanism which does not depend on the manner in which it was formed. The theory as it exists today cannot predict the parameters Γ_n, Γ_x, E_0, and J for the individual resonances. These parameters are determined experimentally, and their values have been compiled in an atlas of neutron cross sections.[17] At the same time, it is the complex, many-particle nature of compound states which leads to the definite behavior established by the statistical theory. The behavior described by this theory deals with the expectation values of the decay widths for decay by the various channels, the distributions of the partial and total widths, and the distributions of the intervals between resonances.

b) Distribution of the distances between resonances with definite values of J^π

During the first two decades of the "neutron era," physicists inferred from the complexity of the compound states that the intervals between resonances were distributed at random, i.e., exponentially. Short distances are the most probable in such a distribution. When Gurevich and Pevsner[18] analyzed the experimental data, however, they observed a "repulsion effect," i.e., a deficiency of short distances in the distance distribution. Wigner[19] solved this problem theoretically, examining the distribution of the differences between the eigenvalues of matrices whose elements are numbers chosen at random from a Gaussian distribution. Wigner derived a distribution

$$P_(x) = \frac{\pi}{2} x \exp\left(-\frac{\pi}{4}x^2\right), \quad \bar{x} = 1, \quad \sigma^2(x) = \frac{4}{\pi} - 1 \quad (5)$$

with $x = S/D$, where S is the distance between "neighbors" in the sequence of resonances with identical values of J^π and $D = \bar{S}$.
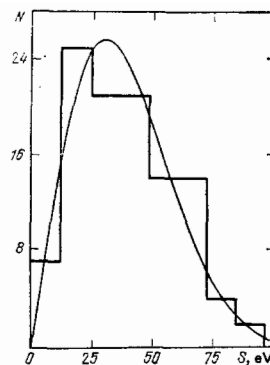

FIG. 2. Distribution of the distances between resonances of erbium-166 (Ref. 20).

This distribution is shown by the solid curve in Fig. 2. The physical reason for the level repulsion is a residual interaction of particles, which has the consequence that the probability for the appearance of a second level in an interval dS at a distance S from the first level is proportional to not only dS/D but also S itself. Not only small but also large distances S are relatively improbable in comparison with a random distribution. The Wigner distribution has been confirmed by many experimental results, e.g., the results obtained on ^{166}Er by a group at Columbia University,[20] shown in Fig. 2.

Subsequently, many other investigators took up the problem, used more accurate methods, and examined various ensembles of random matrices. The corresponding predictions, however, turned out to be very similar to distribution (5), and it is not possible to choose among the various distributions on the basis of the experimental data available. Research on random-matrix theory is summarized in the recent fundamental review by Brody et al.[21]

c) Distribution of widths and their mean values

The widths of the various decay channels of the compound states, λ, are energy-dependent and can be written as follows, according to the R-matrix theory:

$$\Gamma_{\lambda c} = 2\gamma_{\lambda c}^2 P_c, \quad (6)$$

where $\gamma_{\lambda c}^2$ is the energy-independent reduced width, and P_c is the penetrability in channel c, expressed in terms of the Coulomb functions F and G (Ref. 15) as $P_c = R/\lambda(F_l^2 + G_l^2)_c$. For the s-wave neutron widths we have $F_0^2 + G_0^2 = 1$, which leads to an energy dependence $\Gamma_n \sim \sqrt{E}$. It is thus customary to use the quantities $\Gamma_n^0 = \Gamma_n[(1 \text{ eV})/E]^{1/2}$, which are the widths referred to 1 eV. The reduced widths Γ_n^0 and γ_n^2 are related by $\Gamma_n^0 = 2\gamma_n^2 R/\lambda_1$ (λ_1 corresponds to the wavelength of a neutron at an energy of 1 eV). According to the Bohr concept the mean values of the reduced decay widths should not depend on the nature of the final states.

Porter and Thomas[22] have raised arguments for a normal distribution of the amplitudes of the reduced neutron widths γ_n with a mean value $\bar{\gamma}_n = 0$. Their argu-

ments led them to the following distribution of reduced neutron widths:

$$P(y)\, dy = (2\pi y)^{-1/2} e^{-y/2} dy, \quad \bar{y} = 1, \quad \sigma^2(y) = 2, \tag{7}$$

where $y = \gamma_n^2/\langle \gamma_n^2 \rangle = \Gamma_n^0/\langle \Gamma_n^0 \rangle$. In nuclear physics, this distribution has come to be known as the "Porter–Thomas distribution"; in statistics, it is the χ^2 distribution with one degree of freedom ($\nu = 1$). This distribution has been confirmed by several experimental studies, not only for the neutron widths but also for the partial widths of various reactions (Sec. 3). Distribution (7) is very broad; its variance σ^2 is nearly eight times that of distribution (5).

The total widths, which are the sums of the independently fluctuating partial widths, fluctuate far less. For example, the number of degrees of freedom for the total radiation width $\Gamma_\gamma = \Sigma \Gamma_{\gamma i}$ may reach $\nu = 100$ for nuclei with a complex spectrum of final states which result from partial transitions characterized by the partial widths $\Gamma_{\gamma i}$. Recent theoretical results[23,24] on $\langle \Gamma_\gamma \rangle$ reproduce the experimental results fairly well. The experimental information available on the total radiation widths is analyzed in Ref. 25.

In the case of the α decay of neutron resonances, the distribution of the total α widths, which are the sums of the partial widths over the final states f and over the possible orbital angular momenta l, can be described as a χ^2 distribution with an effective number of degrees of freedom

$$\nu_{\text{eff}} = (\Sigma T_{\alpha l f})^2 (\Sigma T_{\alpha l f}^2)^{-1}, \tag{8}$$

where $T_{\alpha l f}$ is the barrier penetrability for the corresponding α transition. According to the statistical theory, the expectation values of the total widths of the various resonances can be evaluated from the following expression, in accordance with the approach taken by Blatt and Weisskopf[26]:

$$\langle \Gamma_c \rangle = \frac{D^{J\pi}}{2\pi} \Sigma T_c(E, l), \tag{9}$$

where $D^{J\pi}$ is the average distance between resonances with spin and parity J^π (this distance is a few electron volts for heavy nuclei), and l is the orbital angular momentum of the emitted particle or the multipolarity of the γ ray. This simple expression was proposed 30 years ago for order-of-magnitude estimates of the mean values of the widths, but a comparison with the most recent experimental data shows that the mean widths can be described considerably more accurately by expressions of the type in (9). The only important point is to calculate correctly the penetrability for the emitted particle, bearing in mind effects which do not occur in the statistical model; for example, the optical model should be used to allow for the semi-transparency of the nucleus for neutrons.

Experimentally, the mean widths are determined by measuring the widths of individual resonances. Because of the large random fluctuations in the widths, however, the accuracy of this averaging procedure is not always good. Since the resolution of neutron spectrometers (more on this below) falls off quite rapidly with the neutron energy, the number of resonances which have been reliably studied for each isotope is limited, generally to a few dozen. For the widths fluctuating in accordance with the Porter–Thomas distribution, the mean width is then subject to an uncertainty of about 20%. More accurate mean widths can be determined by analyzing the average cross sections found by taking averages over hundred or thousands of resonances.

d) Strength function

A concept which has proved extremely fruitful in neutron physics is the strength function, defined by

$$S_c = \frac{2\gamma_c^2}{D} = \frac{\langle \Gamma_c \rangle}{D P_c}. \tag{10}$$

The second equality in (10) follows from (6). In the statistical model, the penetrability P_c should be taken to be the quantity T_c determined by (9). Substitution of this quantity into (10) shows that in this case the strength function should be constant not only over energy but also from one nucleus to another; the observation of a deviation from this rule means that nonstatistical processes are having an effect in the given reaction channel. A slightly different definition has come down over the years for the neutron strength function (for the interaction of s neutrons with nuclei): $S_n^0 = \langle \Gamma_n^0 \rangle / D$. This definition is the same as that in (10) within a factor R/λ_1.

Hughes et al.[27] measured the neutron strength functions by the method of average cross sections and showed that there are giant "size resonances" in the dependence of the strength function on the mass number A (or on R, the size of the nucleus). Figure 3 shows recent data on the s-wave strength function; the corresponding results for the p-wave strength function can be found in the review in Ref. 28.

This behavior of S_0, like the smooth maxima detected previously by Barschall[29] in the cross sections for the scattering of neutrons with energies up to a few MeV, was ascribed to the semitransparency of the nucleus with a corresponding complex potential $V = V_0 + iW_0$ in the Schrödinger equation—in a departure from the

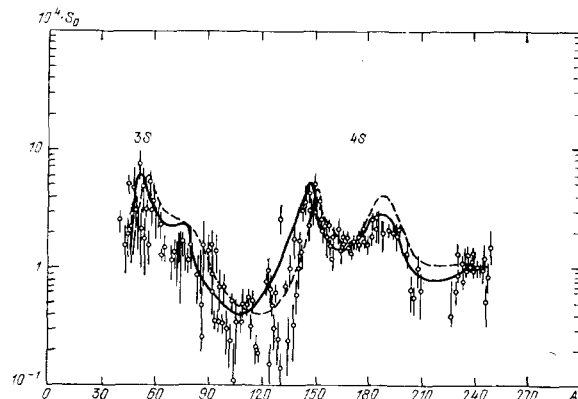FIG. 3. Neutron strength function as a function of the mass number.[17] For the solid curve, the potential of the optical model, V_0, is 43.5 MeV; for the dashed curve it is 41.5 MeV.

301   Sov. Phys. Usp. 25(5), May 1982

Pikel'ner et al.   301

statistical theory. This approach gave rise to the optical model of the nucleus[30],[31] and its modern versions, which incorporate the concept of doorway states (see Ref. 32, for example).

For a long time, the role played by the spin–spin terms V_{0s} and W_{0s} in the optical potential remained unclear. These terms describe the spin dependence of the cross section for the interaction of neutrons with nuclei. Some recent results from experiments with polarized rare earth nuclei and polarized neutrons have yielded $W_{0s} = 0.10 \pm 0.06$ MeV (Ref. 33) and $V_{0s} \leqslant 0.08$ MeV (Ref. 34). The spin–spin terms in the optical potential are thus much smaller than the leading terms ($W_0 \approx 5$ MeV, $V_0 \approx 40$ MeV).

In general, the statistical theory is now capable of correctly predicting the average characteristics of compound states, describing the distribution of the various parameters about their mean values, and correctly describing the smooth dependence of the level density at nuclear excitation energies of the order of 10 MeV. It may be said that there is a correspondence between this picture and the experimental data available for the various decay channels of the neutron resonances.

On the other hand, we know only a rather small number of the conventional characteristics of these very complex compound states: the energy, the spin, the parity, the neutron and total radiation widths, (more rarely) the partial γ widths, and (even more rarely) the α and proton widths. Accordingly, one of the most important problems of the modern neutron spectroscopy of nuclei is to add to the number of characteristics of the neutron resonances which have been studied (for example, to study the electric and magnetic moments and the radii) and to study new decay channels for these resonances. This will generally require detecting weak effects and reactions with extremely small cross sections. It is therefore crucial to raise the intensity of neutron sources, to develop highly efficient detectors and spectrometers for the secondary particles, and to develop a variety of methods for high-intensity spectrometry.

e) General questions of high-intensity neutron spectrometry

Modern neutron spectrometry is capable of resolving individual states of nuclei which are separated by a fraction of an electron volt at a total excitation energy of the order of 7–10 MeV. This resolution—unique in nuclear physics—is achieved by comparatively simple means and stems from the fact that the excitation energy of a compound nucleus is $E^* = B_n + E_n$, where B_n is the binding energy of the captured neutron, which is the order of 10^7 eV, while the spectrometry (usually time-of-flight spectrometry) is carried out at a comparatively low kinetic energy of the neutron, $E_n \leqslant 10^4$ eV.

This relationship between the components of the excitation energy ($E_n \ll B_n$), which is possible only in the case of neutron capture, allows us to study in its pure

form the distinct class of nuclear reactions which go through a compound-nucleus stage and to study the nature of these complex, quasistationary states.

The experimental methods of neutron spectrometry include various methods for producing monoenergetic neutrons or for singling out the effects of monoenergetic neutrons in measurements of the total and partial cross sections for neutron–nucleus interactions. The most important of these methods either use sources of monoenergetic neutrons [nuclear reactions of the type ^{7}Li(p, n) or photoneutron sources of the Sb–Be type] or make it possible to single out monoenergetic neutrons from a source with a continuous neutron distribution (time-of-flight methods, moderation-time methods, nuclear filters, etc.).

Over the past three decades experimental neutron spectroscopy has been improving continually. It has come a long way from the simple chopper selectors in the first nuclear reactors to the modern spectrometers installed at powerful pulsed accelerators of electrons, protons, and deuterons; pulsed reactors; high-flux steady-state reactors; etc.[35],[36]

Neutron spectroscopy is developing along the directions of increasing resolution and increasing intensity. The variety of research programs is forcing improvements in both these major characteristics of neutron spectrometers. The general-purpose spectrometers for experimental physics, however, usually cannot claim record high characteristics, so that many interesting and pioneering studies are being carried out with specialized apparatus. It should also be emphasized here that a successful experiment requires matching the basic characteristics of the neutron spectrometer with those of the particle detectors, those of the system which detects the events, and (in several complex recent experiments) those of the computer facilities. Otherwise record high characteristics may turn out to be useless. Table I illustrates the situation with the characteristics of several time-of-flight neu-

TABLE I. Characteristics of certain pulsed sources for neutron spectroscopy.

Spectrometer	Accel. particle	E_{max}, MeV	I_{peak}, A	Δt, ns	Q, neutrons/s	q, neutrons/pulse	ν, Hz	L_{max}	Ref.
1. SC (New York)	p	385	0.33	20	$2 \cdot 10^{13}$	$3 \cdot 10^{11}$	60	200	35
2. IC (Karlsruhe)	d	50	3	1	10^{14}	$6 \cdot 10^8$	$1.5 \cdot 10^5$	180	35
3. FAKEL (Moscow)	e	60	0.5	50—5000	$2 \cdot 10^{12}$— $4 \cdot 10^{13}$	$2 \cdot 10^{10}$— $4 \cdot 10^{11}$	100	230	37
4. GELINA (Geel)	e	150	9	10	$2.3 \cdot 10^{13}$	$2.3 \cdot 10^{10}$	$0.9 \cdot 10^3$	400	38
5. ORELA (Oak Ridge)	e	140	15	3—30	10^{14}	10^{11}	10^3	200	39
6. HELIOS (Harwell) with booster	p	128	1.0	100	$0.3 \cdot 10^{15}$	$0.76 \cdot 10^{12}$	90	300	40
7. WNR (Los Alamos) without storage ring	e	800	—	0.2—3000	10^{12}— $2 \cdot 10^{11}$	—	120	300	41
8. LUE-40 + IBR-30 (Dubna)	e	40	0.2	4500	$0.3 \cdot 10^{15}$	$0.3 \cdot 10^{12}$	100	1000	42
9. GNEIS (Gatchina)	p	1000	—	10	$2.7 \cdot 10^{14}$	$5 \cdot 10^{12}$	50	45	43
10. IBR-2 (Dubna)	—	—	—	10^5	$1.8 \cdot 10^{17}$	$3.6 \cdot 10^{15}$	50	1000	44

302   Sov. Phys. Usp. 25(5), May 1982

Pikel'ner *et al.*   302

tron spectrometers installed at accelerators and pulsed reactors.

The first column gives the name by which the spectrometer is known in the literature. The abbreviation IC means isochronous cyclotron; SC means synchrocyclotron; E_{max} is the maximum energy of the accelerated particles; I_{peak} is the instantaneous peak value of the current in the pulse; Δt is the pulse length; Q is the total neutron yield per second; q is the neutron yield per pulse; ν is the pulse repetition frequency; and L_{max} is the maximum usable baseline. In principle, this array of spectrometers can deal with a very broad range of neutron-spectroscopy problems, although an even higher intensity is required in certain experiments.

There are several ways to raise the transmission of neutron spectrometers.

1) To increase directly the neutron flux density from the source, without changing the other characteristics of the spectrometer [raising the current (energy) of the accelerated particles or using targets of fissionable materials].

2) To alter the characteristics of the spectrometer. In the time-of-flight method, this would mean increasing the length of the neutron pulse or moving closer to the neutron source. In the latter case it must be kept in mind that a limitation is imposed by the dimensions of the accelerator target (or of the moderator) and of the sample (or of the detector).

3) To use (in the time-of-flight method) a booster or neutron multiplier. This booster can be either a steady-state device (like that at Harwell in England) or a pulsed device (like that used with the IBR-30 fast-neutron reactor at Dubna). At neutron pulse lengths of a few microseconds, this approach can raise the neutron flux density by one or two orders of magnitude.

4) To use moderation-time neutron spectrometry.

f) Time-of-flight method

Neutron sources generally provide neutrons with a continuous energy distribution, and special methods are required to single out neutrons of a particular energy or to measure their energy. The most versatile of these methods is the time-of-flight method. Pulsed operation of the neutron source is convenient for this method. We denote by l the distance (in meters) traversed by the neutron in moving from the source to the detector, by t (in microseconds) the time of flight, and by Δt the uncertainty in this time which results from the finite length of the neutron pulse and other factors. From the nonrelativistic equations $E = mv^2/2$ and $t = l/v$ we can then derive the basic equations of the method:

$$E_n = 5228 \left(\frac{l}{t}\right)^2, \quad \frac{\Delta E_n}{E_n} = 0.028 \sqrt{E_n}\, \frac{\Delta t}{l}. \tag{11}$$

The total cross section is usually determined as a function of the energy, $\sigma_t(E_n)$, by measuring the transmission of neutrons by the sample for various times of flight. The transmission T and the cross section σ_t are related by the simple equation

$$T = e^{-n\sigma_t} \tag{12}$$

The reason that measurements with a uniquely high resolution are possible, as mentioned earlier, is that ΔE_n can be made arbitrarily small by letting $l \to \infty$. At the values used in practice, for example, $\Delta t = 1\ \mu s$ and $l = 100$ m, the uncertainty in the energy is $\Delta E_n = 0.3$ eV at $E_n = 100$ eV and increases with increasing energy in proportion to $E^{3/2}$. For a given duration of the neutron burst, the source intensity places a limit on the improvements in the resolution.

The IBR-30 fast-neutron reactor[42] has been in operation for many years now in the Neutron Physics Laboratory of the Joint Institute for Nuclear Research. The average power of this reactor is 25 kW, and at five pulses per second it generates a pulsed power of 60 MW—matching that of the best steady-state research reactors. For experiments with resonance neutrons, the reactor is operated in a booster mode in combination with an electron injector–accelerator. The accelerator target is placed in the active zone of the reactor, and the neutron pulses produced at the target as the result of a photonuclear reaction are multiplied by the subcritical reactor by a factor of 200. In this mode, the source has an average intensity of $3 \cdot 10^{14}$ neutrons/s at a neutron pulse length of 4.5 μs. By way of comparison, the intensity at the electron accelerators in operation usually does not exceed 10^{14} neutron/s (Table I). A pulsed reactor with an injector is therefore one of the best choices for high-intensity neutron spectroscopy at a modest resolution.

g) Moderation-time neutron spectrometry

This is an interesting method because of the underlying physics and also because of the opportunities it presents the experimentalist. The concept arose from Lazareva, Feĭnberg, and Shapiro's discussions[45] of a particular feature of the moderation process which results from the elastic scattering of neutrons in a heavy medium: the bunching of the neutron velocities in a comparatively narrow interval around an average value. A crude explanation is that the range of the neutron between collisions depends only slightly on the neutron velocity, so that the faster neutrons collide more frequently with the moderator and lose energy more rapidly.

If a brief pulse of fast neutrons at a velocity v_0 is injected into a large volume of a moderator consisting of nuclei with $A \gg 1$, the neutrons will collide elastically with the moderator nuclei, losing an average fraction $\approx 2/A$ of their energy in each collision, and will accordingly accumulate in a comparatively narrow velocity interval. As the moderation time increases, this interval shifts downward along the velocity scale. By operating the neutron detector (or devices which detect particles accompanying the capture of a neutron by a nucleus of the test sample) for a narrow time interval Δt by a time t with respect to the time of the neutron injection, it becomes possible to select approximately monoenergetic neutrons. The average energy of these neutrons is related to the moderation time t by

$$t = A\Lambda \left(\frac{1}{v} - \frac{1}{v_0} \right), \qquad (13)$$

where Λ is the mean free path of the neutron with respect to scattering, and v_0 is the initial velocity of the neutrons. The product $A\Lambda$, which is ~6 m for lead, is an effective "flight distance," by analogy with the time-of-flight method.

This idea was embodied in a moderation-time spectrometer by a group led by Shapiro at the Lebedev Physics Institute in Moscow.[46] The neutron source, with an average intensity of about 10^9 n/s, was a tritium target exposed to a pulsed beam of 300-keV deuterons. The target was placed at the center of a lead prism with dimensions of $2 \times 2 \times 2.3$ m, in which the neutrons were moderated. The detector was inserted into a narrow channel in the prism. This method admittedly has the disadvantage of low resolution ($\approx 30\%$), but it has the undisputed advantage of high transmission. This method is widely used to measure capture and fission cross sections over the energy range from 1 eV to 30 keV (see the papers by Bergman and Popov cited in Ref. 46). A second life was recently breathed into this method at Rensselaer Polytechnic Institute,[47] where a neutron source (the target of an electron accelerator) with an intensity 1000 times higher was inserted into a lead cube. In this case the sensitivity to the measured cross sections for subbarrier fission and the (n, α) and (n, p) reactions amounted to a fraction of a microbarn.

h) Filtered beams

An important technical advance in the past decade was the development and practical implementation of a filter method[48] for producing intense, approximately monoenergetic beams of intermediate-energy neutrons at steady-state research reactors. This method raises the accuracy of measurements of the average characteristics of neutron resonances and permits measurements of smaller cross sections (see Sec. 3). The materials which are used as filters, (iron-56 or scandium, for example) have total neutron cross sections which go through minima at certain energies. These minima result from an interference of resonance scattering and potential scattering. When neutrons are filtered through a thick layer of such a material, the resulting beam has an energy which corresponds to the interference minimum and an energy width ΔE_n determined by the thickness of the filter. The intensity of the neutrons of other energies which remain (the background) is usually 3–6%. Various combinations of these materials with other materials (aluminum, sulfur, and sodium, for example) are used to suppress this background. Table II shows the basic characteristics

TABLE II. Parameters of filtered beams.

Filter	$\bar{E}_n$, keV	ΔE_n, keV	I, neutrons/s
96 cm Sc	2	0.9 (0.6)	$4 \cdot 10^7$ ($2 \cdot 10^6$)
22.9 cm Fe 36.2 cm Al 6.3 cm S	24.3	2.0 (2.1)	$1 \cdot 10^7$ ($1 \cdot 10^6$)

of some of these filters, compiled from the data of Ref. 49. The total intensity I corresponds to a beam working area of 7 cm^2 and reaches the high level of 10^7 neutron/s at the sample, as can be seen from the table. This intensity was achieved at the HFBR high-flux reactor at Brookhaven.

Shown in parentheses here are the values for a standard Soviet VVR-M reactor with a thermal-neutron flux density $\approx 7 \cdot 10^{13}$ neutrons/(cm$^2 \cdot$ s) in the active zone, at the Institute of Nuclear Research of the Academy of Sciences of the Ukr. SSR, Kiev. Filtered beams of this type are widely used there to measure a variety of neutron cross sections.[50]

i) Method of polarized nuclear targets and polarized neutron beams

Most neutron experiments use unpolarized neutrons and unoriented nuclear systems having an isotropic distribution of spin projections onto the quantization axis. This approach frequently loses information on spin-dependent aspects of the neutron–nucleus interaction. There is an exceptional situation at low energies (below 10 eV), where neutron polarization methods based on the spin dependence of magnetic scattering have been developed and used successfully (see Ref. 51, for example). Not until the mid-1960's was a polarization method developed (in the Neutron Physics Laboratory, Joint Institute for Nuclear Research, Dubna[52]) for the broad resonance region of neutron energies ($\lesssim 100$ keV), which made it possible to work with a comparatively low neutron-beam intensity loss. This method makes use of the strong spin dependence of neutron–proton scattering. By passing the primary beam through a polarized proton target, one can filter out one of the two spin components of the beam or, in other words, polarize the beam.

The method which has been adopted most extensively for producing polarized nuclear targets is the method of thermal equilibrium with pronounced cooling in an external magnetic field. The magnetic fields and low temperatures required here can be attained under laboratory conditions because of recent advances in superconducting magnets and cryostats in which helium-3 is dissolved in helium-4. Another possibility is to use intraatomic "hyperfine" magnetic fields, as a Dubna group has done.[53]

Polarization experiments are an extremely high-intensity method for studying many weak effects, e.g., parity nonconservation and the spin-dependent intermediate structure in the cross sections. We might also note that the polarization method is a direct method for identifying the spins of neutron resonances. As is illustrated in Fig. 4 for a terbium target, it is sufficient here to determine the sign of the polarization effect, ε, defined as the relative difference between the detector count rates when the polarization of the neutrons and the nuclei are parallel and antiparallel.

j) Progress in high-transmission detection apparatus

The increases in the intensity of the neutron sources have been accompanied by refinements in the apparatus
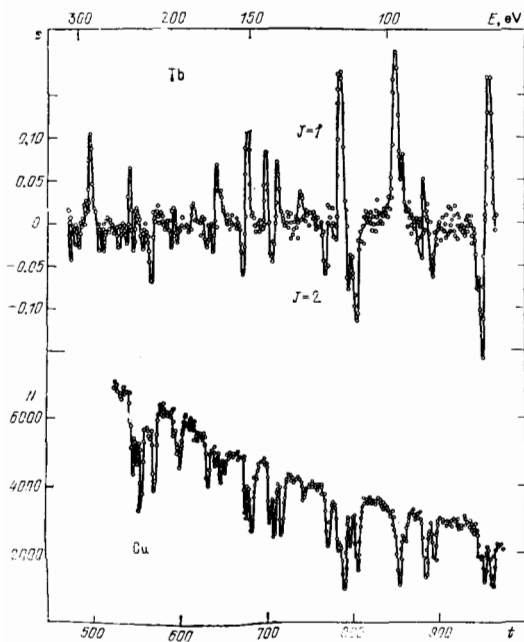
FIG. 4. Bottom—experimental transmission spectrum of terbium, plotted against the time of flight, t; top—the polarization effect ε, which determines the spins of the resonances.[53]
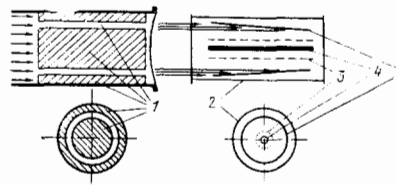

FIG. 5. Schematic diagram of high-transmission ionization chamber (2) and of a neutron collimator (1). 3—grid; 4—collector; 5—sample.

used to detect the products of the neutron–nucleus reactions. Harvey and Hill[54] have published a comprehensive review of modern methods for detecting neutrons by means of scintillators. Semiconductor detectors and spectrometers are finding progressively more experimental applications.[58] They are particularly promising in the spectrometry of the γ rays from the radiative capture of neutrons. The good energy resolution and high efficiency for γ detection of germanium semiconductor spectrometers, combined with a time-of-flight procedure, have finally made it possible to study the properties of the partial γ transitions for a broad range of individual neutron resonances. They have also made it possible to study some interesting aspects of the mechanism for the radiative capture of neutrons.[11]

Semiconductor charged-particle spectrometers are widely used in measurements with thermal neutrons, which are available in extremely high flux densities in advanced research reactors. In studies of the charged particles produced in reactions with resonance neutrons (where the flux densities are many orders of magnitude lower than those for thermal neutrons), semiconductor detectors and spectrometers, with a sensitive area no greater than 10 cm^2, run into rough competition from modern ionization and proportional chambers. Although ionization spectrometers have a resolution which is poorer by a factor of several units, their sensitive area (or their efficiency) is larger by two or three orders of magnitude. Studies of the α spectra for individual resonances and studies of the average partial cross sections in the reaction (n, α) and $(n, \gamma\alpha)$ have become possible only by combining special ionization chambers having a large sensitive area with a high-

transmission neutron spectrometer, used with a linear electron accelerator with a pulsed booster–breeder in the form of an IBR fast-neutron pulsed reactor (Sec. 3).

Figure 5 is a schematic diagram of one such ionization chamber,[56] with a target area of $3 \cdot 10^3$ cm^2. The collimation system for the neutron beam and the shape of the target (sample) are chosen to minimize the bombardment of the sensitive volume of the ionization chamber with neutron and γ rays from the source while the entire target is being bombarded. This approach has made it possible to raise the resolution of the spectrometer by a factor of several units and to extend the working range of times of flight in operation with an intense neutron source and comparatively short baselines.

Some new possibilities for neutron-spectroscopy research have been opened up by the experimental approach known as "multiplicity spectroscopy."[57] The idea here is not to measure the average number of radiative-capture γ rays but to measure the distribution in the multiplicity of all particles and γ rays emitted during absorption of the neutron by the nucleus. Figure 6 shows a schematic γ multiplicity spectrum of this sort, $N_{\gamma}(\nu)$. The readings at $\nu = 1$ correspond to the scattered neutrons which are detected by a special neutron–gamma converter, which produces one γ ray for every neutron which it captures. The peaks at $\nu \approx 3$ and $\nu \approx 9$ are determined, respectively, by radiative capture and by fission, detected from the accompanying γ rays. It is thus possible to detect simultaneously all three basic processes which result from the inter-
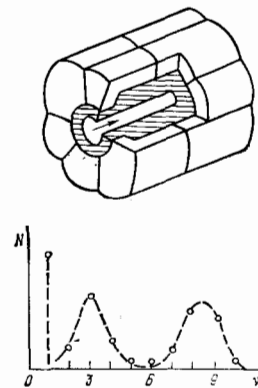

FIG. 6. Bottom—schematic multiplicity spectrum; top—$4\pi\gamma$ detector.

action of neutrons with heavy nuclei. Furthermore, by analyzing the differences in the shape of the multiplicity distributions of the γ rays corresponding to radiative capture of neutrons in the various resonances, one can identify the spins of the resonances. An apparatus for γ multiplicity spectrometry has been developed at the Kurchatov Institute of Atomic Energy, Moscow. This is a 4π high-transmission γ-detector, consisting of 46 independent NaI(Tl) crystals with a total volume ≈ 100 liters with an electronic system for recording two-dimensional information.

Now that we have reviewed the basic aspects of the interactions of resonance neutrons with nuclei and certain methodological aspects of modern neutron research, we will move on to the experimental results on some new characteristics of neutron resonances which have been obtained primarily through the development of high-intensity methods of neutron spectroscopy of nuclei.

3. α DECAY OF COMPOUND NUCLEI

There are two motivations for studying the reaction (n, α) with resonance neutrons. On the one hand, this is a new approach in neutron spectroscopy, which can furnish information on the total and partial α widths: a set of characteristics of the neutron resonances which complements the known neutron and radiative widths. On the other hand, this is a new type of α decay: the decay of very complex, highly excited compound states. Since the lifetimes of these states are many orders of magnitude longer than the nuclear scale times, as we have already noted, they may be treated as approximately stable states, and we may speak in terms of the α decay of neutron resonances, by analogy with the well-known α decay of ground states.

In several cases, study of the α decay of compound states makes it possible not to get involved in the individual structural features of the decaying state and to expand greatly the range of α-decay energies which can be studied. For the ^{144}Nd nucleus, for example, the energy of the α decay of the ground state is $E_\alpha^0 = 1.8$ MeV, while for compound states (because of the addition of the neutron binding energy) the decay energy is $E_\alpha^c = 9.4$ MeV. The result is a difference by 33 orders of magnitude between the decay half-lives of the ground and compound states of ^{144}Nd. Furthermore, the reaction (n, α) makes it possible to extend the use of α decay—one of the "ancient" tools for studying nuclear structure and various aspects of the dynamics of intranuclear processes—to new nuclei and even to a new range of nuclei, with $A < 120$.

At the same time it must be noted that the reaction (n, α) in heavy and intermediate nuclei with slow neutrons is significantly suppressed because of the low penetrability of the Coulomb barrier of the nucleus, since the energy of the emitted α particle is less than or equal to the energy of the Coulomb barrier: $E_\alpha \leqslant E_{Coul}$. The cross sections for the (n, α) reaction have proved to be very small; if, for example, we compare them with those for the well-studied radiative capture of a neutron we find that the ratio $\sigma(n, \alpha)/\sigma(n, \gamma)$ is only

10^{-3}–10^{-5}, even under the most favorable conditions. This circumstance is responsible for many methodological difficulties and explains the relatively late development of this direction in neutron spectroscopy.

Such aspects of the (n, α) reaction as the cross sections, the large background from the competing reaction (n, γ), and the short range of α particles in the target material impose specific requirements on the method for studying this reaction. It is important that the neutron spectrometer have a high transmission and that the bombardment target have a large area. These are particularly important considerations in experiments with resonance neutrons, whose flux densities are several orders of magnitude lower than those of thermal neutrons in modern research reactors. As a result, while semiconductor detectors with an area of 1 cm^2 are commonly used to measure the α spectra in the reaction (n, α) with thermal neutrons, for measurements with resonance neutrons it has proved extremely useful to combine a "slow" (microsecond-range) but high-transmission time-of-flight neutron spectrometer, used with a fast-neutron pulsed reactor, with the highly efficient α detectors and spectrometers described in Sec. 2.

Study of the reaction (n, α) with heavy and intermediate nuclei, i.e., study of the α decay of compound nuclei, began 20 years ago with the studies of thermal neutrons by Macfarlane and Almodovar[58] and Chiefetz et al.[59] Experiments with thermal neutrons, however, yield only fragmentary information on the decay of compound nuclei, since (a) the characteristics of the decaying states frequently remain undetermined (whether the cross section for the given reaction with thermal neutrons can be ascribed to a "tail" of an individual resonance or whether several resonances contribute cannot always be determined) and (b) the results are a random sampling of the values of the individual parameter from the broad Porter–Thomas distribution. At the same time, analysis of data on thermal neutrons for a range of nuclei sometimes yields some interesting qualitative conclusions. For example, Andreev and Sirotkin[60] analyzed the results of their search for the reaction (n, α) in several nuclei and reached the conclusion that the usual one-particle model for α decay does not apply here and that the α decay of compound nuclei is described better by the statistical model. This conclusion received quantitative support a few years later, when the first experiments on the reaction (n, α) with resonance neutrons were begun at Dubna.[61,62]

The first step was to search for the reaction (n, α) among the resonances of various nuclei. A time-of-flight method and high-transmission detectors were used to determine the α yield and total α widths of the neutron resonances.[63] In the second step, two-dimensional measurements were carried out for the nuclei and resonances having the maximum α yield; specifically, the time of flight and the spectrum of the detected α particles were determined for each time channel. In this manner, the partial α widths were determined for each resonance.[62]

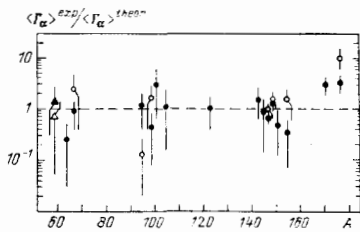306   Sov. Phys. Usp. 25(5), May 1982

Pikel'ner et al.   306

FIG. 7. Ratio of the experimental and theoretical values of the average α widths, plotted against the mass number of the nucleus.

FIG. 8. Strength functions for the reaction ^{147}Sm(n,α), as a function of the neutron energy.

In addition to research on the α decay of individual neutron resonances, recent years have seen advances in the measurements of the characteristics of the (n,α) reaction, averaged over many resonances, through the use of "quasimonoenergetic" neutron beams passed through nuclear filters[65] (discussed above) and also the time-of-flight method. These methods are employed when the energy resolution of the neutron spectrometer is inadequate to resolve the individual resonances.[56]

We turn now to an analysis of the experimental data available.

a) Average α widths

Figure 7 shows ratios of the average total α widths found experimentally to those calculated from Eq. (9) with the attachment coefficients taken from the Kadmenskiĭ–Furman cluster model.[64] The errors result primarily from the limited number of resonances over which the experimental α widths are averaged. We can conclude from Fig. 7 that the statistical theory satisfactorily reproduces the average total α widths for a broad range of spherical nuclei, with $58 \leqslant A \leqslant 150$. The discrepancies in the region of deformed nuclei may be a consequence of the neglect of the nuclear deformation in the calculation of $\langle\Gamma_\alpha\rangle^{\text{cl}}$.

Since the theoretical value of $\langle\Gamma_\alpha\rangle^{\text{cl}}$ was calculated from (9), the ratio $\langle\Gamma_\alpha\rangle^{\text{exp}}/\langle\Gamma_\alpha\rangle^{\text{cl}}$ in Fig. 7 is, within a factor, the strength function for α particles [see expression (10)]. The fact that the strength function S_α remains constant for spherical nuclei, as we see from this figure, may be interpreted as evidence of strong absorption of α particles in the nucleus (in other words, the correct model would be a "black" nucleus, rather than a semitransparent one, as in the case of neutrons). If this is the case, then it follows that the α-cluster states are highly fragmented (distributed) among the levels of a compound nucleus at nuclear excitation energies ≈ 10 MeV.

A further test of the conclusion that there are no giant "optical" resonances for the α channel might be to analyze the energy dependence of the average cross sections for the (n,α) reaction at energies of the order of 1 MeV. The experimental data available, however, permit such an analysis only up to ≈ 30 keV. Figure 8 shows the energy dependence of the experimental values of $\langle\Gamma_\alpha/D\rangle_{J\pi}$ in the reaction ^{147}Sm(n,α), obtained in experiments by Dubna and Kiev groups.[65] Here the indicated errors reflect the limited numbers of reso-
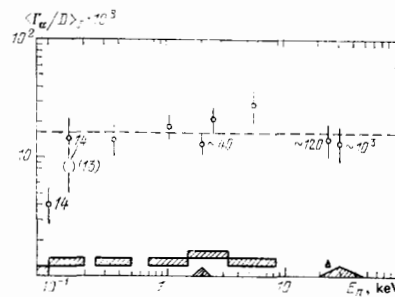
nances (the numbers beside the points) over the averaging intervals. The averaging intervals themselves are shown by the hatched bars near the bottom of the figure. Shown in parentheses for the interval 100–200 eV is a result obtained without consideration of the anomalous resonance at $E_0 = 184$ eV, which has a "high affinity" for the α and neutron channels.[66] The constancy of the experimental ratios $\langle\Gamma_\alpha/D\rangle_{J\pi}$ may be interpreted as proof that the statistical approach is valid for describing the reaction (n,α) and as proof that intermediate structures have no effect.

b) Distribution of α widths

Figure 9 shows the integral distribution of partial α widths for transitions to the ground state in the reaction ^{123}Te$(n,\alpha)^{120}$Sn. The experimental errors were incorporated in the determination of $\Gamma_{\alpha0}$ by taking values of the latter from a Gaussian distribution with a half-width equal to the measurement error. The experimental curve (the solid curve) turns out to agree well with the Porter–Thomas distribution (the dashed curve). A similar agreement can be demonstrated for other nuclei.

We can also study the distributions of the total α widths, comparing them with a χ^2 distribution with the value of ν_{eff} calculated from (8). Figure 10, from Ref. 67, shows that the experimental distributions of the total α widths (the histograms) agree well with the theoretical distributions (the solid curve) for resonances of both spins in the case of the compound nucleus ^{148}Sm. The agreement is particularly good if we discard the anomalous resonance at $E_0 = 184$ eV (the dashed curve).

It would be extremely interesting to make a comparison in the region of deformed nuclei, where the most
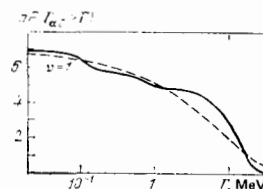

FIG. 9. Integrated distributions of the partial α widths for the reaction ^{123}Te(n,α). Dashed curve—theoretical; solid—experimental.
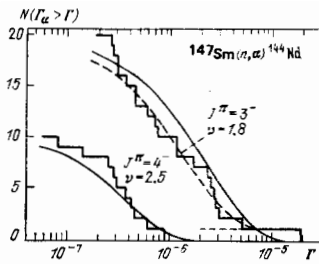
FIG. 10. Distribution of the total α widths.

intense α transitions go to levels of the rotational ground band. If the rotational components play a significant role in the wave function of the compound state, then this circumstance may lead to a correlation of the α transitions to various levels of the same rotational band and thus to a value of ν_{eff} lower than that calculated from (8).

c) α transitions to various final states

According to the statistical theory, which gives a satisfactory description of the basic properties of neutron resonances, the nature of the final states should not affect the average probabilities for the α decay of compound nuclei. In other words, the reduced α widths for decay to various final states, averaged over the initial states with identical spins and parities, should be identical. At the same time, a semimicroscopic approach suggests a possible enhancement of the probabilities for α transitions to one- and two-phonon states in comparison with the α transition to the ground state for even–even final nuclei.[68] Work in this direction was summarized in Ref. 69, where a Monte Carlo method was used to study the intensity ratios of α transitions to the ground and excited states in the reaction $^{147}Sm(n,\alpha)^{144}Nd$ for various neutron energy intervals, in the statistical theory. Figure 11 shows some representative results on the distributions of the quantities $R = N_{\alpha 1}/N_{\alpha 0}$ found in a "mathematical experiment" of this type for four of the six energy intervals studied (the histogram), along with experimental values R_{exp}. For all six intervals (independent results), R_{exp} is displaced from the peak of the theoretical distribution. After analysis of all the data available, it was concluded in Ref. 69 that, with a confidence level of 99.92%, there is a slight enhancement of the reduced probabilities for α transitions to one- and two-phonon states in comparison with the α transition to the ground state of the daughter nucleus. Future experiments may reveal the nature of this enhancement—whether it is (1) a "remnant" of the enhancement due to the appearance of many-quasiparticle components of the wave functions in the final states, as predicted by Solov'ev,[68] (2) perhaps an error in our description of the penetrability of the nuclear barrier over an energy interval ~0.5 MeV, or (3) perhaps simply a random fluctuation in the partial widths.

d) Measurements with thermal neutrons

Emsallem[70] has recently reported a detailed analysis of measurements of the reaction (n, α) with thermal
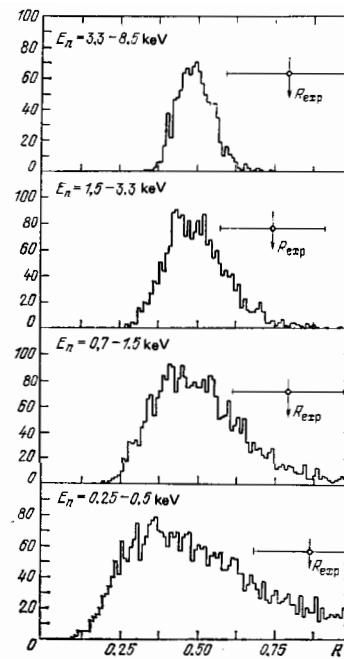

FIG. 11. Ratio R of the intensities of α transitions to the ground and excited states in the reaction $^{147}Sm(n, \alpha)$ and comparison with the statistical theory.

neutrons. Comparison of the thermal cross sections with the results of a calculation of the contribution of the known resonances to the thermal region showed that the calculations and the measured results for most nuclei either were in agreement or differed in a way which could be ascribed to bound states of "negative" resonances, with plausible α and γ widths. In three cases there are discrepancies which require further study.

A dramatic situation has developed in a study of the (n, α) reaction in the actinide region. The thermal cross section for the reaction $^{238}U(n, \alpha)$ found by a group of physicists (Asghar et al.[71]) at Grenoble leads to a value for Γ_α which is six orders of magnitude larger than that calculated from the statistical theory, although the corresponding calculations in the region $59 \leqslant A \leqslant 177$ agree well with experiment (Fig. 7).

Wagemans et al.[72] recently undertook a new attempt to search for the (n, α) reaction in the various isotopes of uranium. They found negative results for ^{233}U and ^{235}U targets. For $^{238}U(n, \alpha)$ they report a cross section of 1.5 ± 0.5 μb with thermal neutrons. This cross section agrees with that reported by Asghar et al.[71] but the energies of the α particles attributed to this reaction by the two groups differ by 0.5 MeV, which goes far beyond the experimental errors. We could use some new experiments here. If such a high value of Γ_α is confirmed, it might substantially change our understanding of the α decay of heavy compound nuclei.

e) The (n, $\gamma\alpha$) reaction and γ transitions between compound states

One possible decay made of compound states is the emission of a γ ray followed by the α decay of the re-
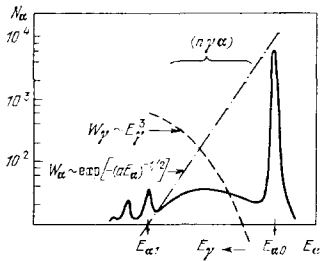
FIG. 12. Schematic energy distribution of α particles in the presence of the $(n, \gamma\alpha)$ reaction.

sulting intermediate state. It is a simple matter to understand at a qualitative level the energy distributions of the γ rays and α particles emitted in a two-step process of this sort. The γ-emission probability W_γ increases with increasing energy E_γ, but at the same time there is a decrease in the energy of the α particles $(E_\gamma + E_\alpha = \text{const})$, which reduces the probability for the emission of an α particle (W_α). Figure 12 is a schematic plot of the α energy distribution. Along with the narrow peaks which correspond to direct α transitions to the ground state $(E_{\alpha 0})$ and the excited states $(E_{\alpha i})$ of the final nucleus in the reaction (n, α_0), there is a broad maximum, caused by a $\gamma - \alpha$ process, whose shape is determined by the product of probabilities $W_\gamma \cdot W_\alpha$. Since a large number of intermediate states participate in the two-step $\gamma - \alpha$ process, there is good averaging over the probability for this process, so that quite general conclusions can be drawn regarding the properties of the intermediate states and the characteristics of the $C - C'\gamma$ transitions, by studying one or two resonances or even the tail of a resonance in the thermal region.

The $(n, \gamma\alpha)$ reaction with thermal neutrons was first observed in the ^{143}Nd nucleus[73] and was regarded by the investigators as an exotic version of the (n, α) reaction. Furman et al.,[74] however, showed that the $(n, \gamma\alpha)$ reaction is a unique source of information about γ transitions between complex, highly excited nuclear states. Information of this sort cannot be extracted from the γ energy distributions during the radiative capture of neutrons because it is impossible to distinguish experimentally the first and subsequent γ rays in the decay of the excited states of heavy nuclei. To some extent, this situation is a consequence of the complexity of the energy distribution of γ rays at energies ≤ 1 MeV, because of the high nuclear state density near the neutron binding energy.

The probability for a γ transition with an energy ≈ 1 MeV between complex, highly excited nuclear states may be determined by essentially any complex component of the wave functions of compound states. The nature of these γ transitions $(C - C'$ transitions) may thus be completely different from that in the case of γ transitions between low-lying states $(S - S'$ transitions: the domain of classical γ spectroscopy) or hard γ transitions between complex and simple states $(C - S$ transitions), which are studied in the radiative capture

of neutrons and protons and which are ascribed primarily to the decay of giant dipole resonances.

Are the $C - C'\gamma$ transitions also determined by giant multipole resonances, or does the effect of such resonances become so small at a distance from the peak equal to a few widths that some other, new, mechanism for γ transitions can manifest itself? This is one of the many questions which have arisen in research on the $(n, \gamma\alpha)$ reaction.

f) Procedure for analyzing experimental data

The partial width for the two-step decay of a state λ_0 to an intermediate state λ_i to the ground state of the final nucleus, accompanied by the emission of a γ ray and then of an α particle (Fig. 1), may be written as follows:

$$\Gamma_{\gamma\alpha_i}(\lambda_0 \to \lambda_i \to 0) = \Gamma_\gamma(\lambda_0, \lambda_i) \sum_{l_\alpha} \frac{\Gamma_{\alpha\lambda_i}(E_\alpha, l_\alpha)}{\Gamma_{\lambda_i}}. \qquad (14)$$

We will take the average of this expression over a comparatively narrow interval $\Delta \ll E_\alpha$ of intermediate states, in which we may ignore the dependence of $\langle \Gamma_\alpha \rangle$ on E_α and that of $\langle \Gamma_\gamma(\lambda_0, \lambda_i) \rangle$ on $E_{\gamma i} = E_{\alpha_0} - E_{\alpha_i}$. For $\langle \Gamma_\alpha \rangle$ we can then use expression (9), which has been verified experimentally.

The average partial width of the first γ transition can be written as the Weisskopf one-particle estimate of the probability for a γ transition of multipolarity l_γ,

$$S^W(E_\gamma, l_\gamma) \sim E_\gamma^{2l_\gamma + 1}, \qquad (15)$$

divided by the forbiddenness $HF(l_\gamma)$, in the approach taken by Lobner[75] in an analysis of data from nuclear spectroscopy:

$$\langle \Gamma_\gamma(\lambda_0, \lambda_i) \rangle = \sum_{l_\gamma} \frac{S^W(E_\gamma, l_\gamma)}{HF(l_\gamma)}. \qquad (16)$$

The total width of a state λ_i which lies below the neutron binding energy B_n can be written as follows if $E_\gamma \ll B_n$:

$$\langle \Gamma_{\gamma\lambda_i} \rangle = \Gamma_\gamma(B_n) \left(1 - \frac{E_{\gamma i}}{B_n - \delta}\right)^n, \qquad (17)$$

where $\Gamma_\gamma(B_n)$ is the total radiation width of the neutron resonances, δ is the pairing energy, and the exponent n lies in the range $1 \leq n \leq 3.5$, just where depending on the particular systematics adopted for the total radiation widths.[23-25] As matters stand at the moment, we can apparently set $n = 2$.

Of interest for comparison with experiment are the total widths $\Gamma_{\gamma\alpha}$, which is the sum of expressions (14) over the intermediate states λ_i, and the shape of the α energy distribution in the $(n, \gamma\alpha)$ reaction, i.e., $N_{\gamma\alpha}(E_\alpha)$, averaged over intervals Δ:

$$N_{\gamma\alpha}(E_\alpha)_j = \frac{\Delta}{2\pi\Gamma_\gamma(B_n)}\left[\sum_{l_\gamma} \frac{S^W(E_\gamma, l_\gamma)}{\{1 - [E_\gamma/(B_n - \delta)]\}^n HF(l_\gamma)} \sum_{l_\alpha} T_{\alpha l}(E_\alpha)\right]_j, \qquad (18)$$

$$\Gamma_{\gamma\alpha} = \frac{\Delta}{2\pi\Gamma_\gamma(B_n)} \sum_j \left[\sum_{l_\gamma} \frac{S^W(E_\gamma, l_\gamma)}{\{1 - [E_\gamma/(B_n - \delta)]\}^n HF(l_\gamma)} \sum_{l_\alpha} T_{\alpha l}(E_\alpha)\right]_j, \qquad (19)$$

where j specifies the averaging interval.

g) Experimental data on C–C' transitions

The very first analysis of the shape of the energy distribution of α particles from the $(n,\gamma\alpha)$ reaction, by Furman et al.,[74] revealed that the average width of soft C–C'γ transitions in the compound nucleus ^{144}Nd has the behavior [see (18)]

$$\langle \Gamma_\gamma(\lambda_0, \lambda_i) \rangle \sim E_\gamma^3. \tag{20}$$

We thus have $l_\gamma = 1$, and the multipolarity of the C–C'γ transitions may be either M1 or E1, under the condition HF = const. This result was subsequently verified by other studies.

At the same time, these results show that experiments are inconsistent with the assumption that the C–C'γ transitions are caused by a tail of a giant dipole resonance with a constant width, since in this case we should have

$$\langle \Gamma_\gamma(\lambda_0, \lambda_i) \rangle \sim E_\gamma^5. \tag{21}$$

Aldea and Seyfarth[76] recently undertook a new effort to determine the multipolarity of the C–C'γ transitions in the reaction ^{143}Nd$(n,\gamma\alpha)$. They measured the shape of the α energy distribution with a much better statistical accuracy than in other studies, and they analyzed this shape by the least-squares method, allowing for fluctuations of the partial γ and α widths and assuming that only E1 and M1 γ transitions were involved. As the unknown parameter they determined the ratio of forbiddenness factors HF(E1)/HF(M1). Aldea and Seyfarth found the best description of the experimental points with HF(E1)/HF(M1) $\geq 10^4$; i.e., the M1 multipolarity is predominant in the C–C' γ transitions. The resulting description is shown by the dashed curves in Fig. 13(a); the corridor between these curves is a consequence of fluctuations in the partial α and γ widths. The solid curves correspond to the case in which the forbiddenness for the first γ transitions is assumed to depend on the energy in accordance with HF(M1)$\sim E_\gamma$.

These results must apparently be approached cautiously, however, since in analyzing the shape of the α energy distribution Aldea and Seyfarth[76] ignored the energy dependence of the total width of the intermediate states, Γ_{λ_i} [they set $n=0$ in (17)], as had been done previously in a crude analysis of the α energy distributions from the $(n,\gamma\alpha)$ reaction. The solid curve in Fig. 13(b) shows the results of an effort to describe Aldea and Seyfarth's data by expression (20) with $n=1$,
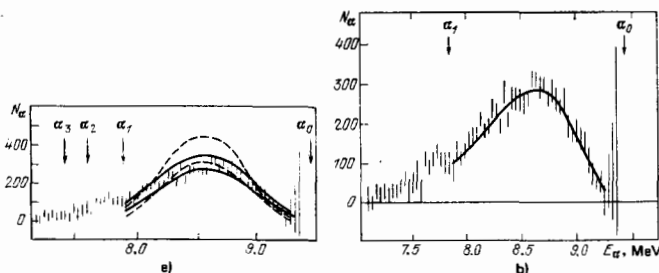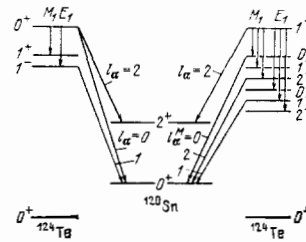

FIG. 14. Scheme of α transitions in the reaction ^{123}Te$(n,\gamma\alpha)$.

HF = const, and $\langle \Gamma_\alpha(\lambda_0, \lambda_i) \rangle \sim E_\gamma^3$. The theoretical curve is drawn to enclose the same area as the experimental data. The agreement is good.

There is yet another possibility for determining the multipolarities of C–C' γ transitions. Analysis of the scheme for the filling of the intermediate states λ_i in the $(n,\gamma\alpha)$ reaction for resonances with various spins reveals that the ratio of widths $\Gamma_{\gamma\alpha}$ for them depends on the assumption made regarding the multipolarity of the first γ transitions. For example, for ^{123}Te resonances with $J^\pi = 0^+$ in the case of the multipolarity M1, the $(n,\gamma\alpha_0)$ reaction is forbidden by parity and angular momentum conservation, but it is allowed in the case of the multipolarity E1 (Fig. 14).

In the case of the reaction ^{143}Nd$(n,\gamma\alpha_0)$ the ratio of widths $\Gamma_{\gamma\alpha}$ for $J^\pi = 3^-$ and 4^- varies by a factor of five, depending on the assumption made regarding the multipolarity of the C–C' γ transitions.[14] Comparison of the results of recent measurements[77] of $\Gamma_{\gamma\alpha}(4^-)$ in the resonances at $E_0 = 55.4$ eV and 159.4 eV with the value found for $\Gamma_{\gamma\alpha}(3^-)$ in the thermal region[71,76] suggests that the multipolarities M1 and E1 make identical contributions (within 30%) to the C–C' γ transitions. We note that in the region of hard γ transitions the intensities of the M1 transitions are, on the average, an order of magnitude lower than those of E1 transitions in this region of mass numbers.[78]

It is worthwhile to compare the probabilities for C–C' radiative transitions with the hard C–S γ transitions, which have been studied in much more detail, in terms of strength functions:

$$S_\gamma(l_\gamma) = \frac{1}{D}\left\langle \frac{\Gamma_\gamma}{E_\gamma^{2l_\gamma+1}} \right\rangle = \frac{1}{D}\frac{S^W(E_\gamma, l_\gamma)}{HF(l_\gamma) E_\gamma^{2l_\gamma+1}}. \tag{22}$$

Figure 15 shows data on $S_\gamma^{CC'}$ obtained in studies of the $(n,\gamma\alpha)$ and $(n,\gamma f)$ reactions (the triangles and squares,

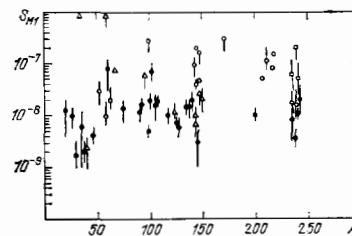FIG. 13. Experimental and theoretical distributions of α particles from the reaction ^{143}Nd$(n,\gamma\alpha)$.

FIG. 15. Radiative strength functions for M1 transitions, plotted against the mass number of the nucleus.

respectively) and data on S_γ^{CS} (the filled and open circles)[79] for M1 γ transitions, plotted against the mass number. There are two interesting points to be noted: the approximate equality of $S_\gamma^{CC'}$ (M1) and S_γ^{CS} (M1) and their weak dependence on the mass number. The latter circumstance seems to allow some rough estimates of the cross section of the (n,$\gamma\alpha$) and (n, γf) reactions.

This is the present state of experimental data on soft γ transitions between compound states.

h) Theoretical aspects of the (n, $\gamma\alpha$) reaction

Attempts to derive a theoretical description of the probabilities for C–C' γ transitions often involve extrapolating the properties of the C–S transitions, which have been studied in more detail, to low energies. When this approach is taken, however, it must be kept in mind that (first) the energy of the C–C' γ transitions lies several widths away from the peak of the giant electric dipole resonance (which can be ascribed for the most part to C–S γ transitions), so that a reliable parametrization of the shape of the giant dipole resonance is important, and (second) the γ transitions with energies ~1 MeV occur within a single shell, so that there may be an enhancement of the one-particle γ transitions between states of the same parity. In other words, there may be an enhanced role of M1 γ transitions.[80,81]

The involvement of many-quasiparticle components of the wave functions of highly excited nuclear states in C–C' γ transitions has been discussed at a qualitative level by Solov'ev (Soloviev).[82] He pointed out that these components will become progressively more important with increasing excitation energy of the nucleus and that it may be possible to observe γ transitions of this nature with intensities comparable to those of one-particle γ transitions.

Kadmenskiĭ et al.[81] have recently attempted to derive a quantitative description of the probabilities for C–C' γ transitions. Taking the approach mapped out by Bunakov and Ogloblin,[83] they showed that by associating the C–C' transitions with the leading components of the wave functions of highly excited states it was possible to derive quite realistic estimates (Fig. 15) of the radiative strength functions for the multipolarity M1 for nuclei with $A \approx 150$:

$$S_\gamma^{C-S} (M1) \approx S_\gamma^{C-C'} (M1) = 2 \cdot 10^{-8} \, \text{MeV}^{-3}.$$

Kadmenskiĭ et al.[81] believe that the contribution of the E1 γ transitions to the C–C' transitions is of a different nature—that these transitions result from small components of the wave functions but are enhanced by the fragmentation of a giant dipole resonance. Calculations for $E_\gamma = 1$ MeV yielded $S_\gamma^{C-C'} \approx 2 \cdot 10^{-8}$ MeV^{-3}, but Kadmenskiĭ et al. regard this value as more of an upper limit on $S_\gamma^{C-C'}$ (E1), because of the uncertainty in the extrapolation of the tail of the giant dipole resonance to such low energies.

4. HYPERFINE-INTERACTION EFFECTS IN NEUTRON RESONANCES

One of the new directions in research on compound states formed in the capture of resonance neutrons arose in recent years from the observation of hyperfine-interaction effects in neutron resonances. Back in its day, research on the hyperfine structure in optical spectra yielded the magnetic moments of stable nuclei. The discovery of the Mössbauer effect—the recoilless emission and absorption of γ rays—attracted much interest to hyperfine interactions and made it possible to measure the magnetic moments and isomer shifts of low-lying excited nuclear states. An important point here was that the width of the γ line observed experimentally was comparable to or less than the energy of the hyperfine interaction. For neutron resonances the situation is much more complicated because of the larger level widths; nevertheless, results obtained in recent years have added significantly to our understanding of highly excited nuclear states.

a) Magnetic moments of compound nuclear states

None of the existing methods for measuring the magnetic moments of excited nuclear states could be used for compound states with excitation energies of 6–8 MeV and lifetimes of the order of 10^{-15} s.

Shapiro[84] was the first to raise the possibility of measuring the magnetic moments of neutron resonances. He suggested determining the magnetic moments from that energy shift of the neutron resonances which results from the hyperfine interaction between magnetic moment of the nucleus and the intraatomic magnetic field, in experiments with polarized neutrons or polarized nuclei.

Let us examine the magnitude of this shift and the mechanism for its occurrence. For a target nucleus with a spin I, a spin projection m, and a magnetic moment μ_0, the imposition of a magnetic field H causes an energy state to change by an amount $\mu_0 Hm/I$. A corresponding shift occurs for a compound state of a nucleus after the capture of a neutron. The resultant change in the energy of a transition between the states under consideration is

$$\Delta E_{mm'} = -H \left(\mu_b \frac{m'}{J} - \mu_0 \frac{m}{I} \right). \tag{23}$$

To derive a final expression describing the shift of a neutron resonance, ΔE_0, it is necessary to sum $\Delta E_{mm'}$ over all possible states, allowing for the statistical weights and populations of the sublevels:

$$\Delta E_0 = \sum_{m, m_s} W(m) W(m_s) (Ism m_s/JM)^2 \Delta E_{mm'}; \tag{24}$$

here $(Ism m_s/JM)$ is the Clebsch–Gordan coefficient. The relative population of a level of the target nucleus with spin projection m may be written

$$W(m) = c \exp \left(\frac{\mu_0 H}{kT} \frac{m}{I} \right). \tag{25}$$

The population $W(m)$ can be related to the nuclear polarization f_N by

311   Sov. Phys. Usp. 25(5), May 1982

Pikel'ner *et al.*   311

$$\sum_m mW(m) = \langle m \rangle = If_N. \qquad (26)$$

For the neutron spin projection m_s, the statistical weight $W(m_s)$ can be expressed in terms of the neutron polarization f_n:

$$W\left(\pm \frac{1}{2}\right) = \frac{1}{2}(1 \pm f_n). \qquad (27)$$

The normalization condition for (24) is

$$\sum_{m,\, m_s} W(m, W(m_s)(Ismm_s|JM)^2 = 1. \qquad (28)$$

Using (25)–(28), we can derive an expression for the shift ΔE_0. In its general form, this is a rather complicated expression, but in practice one can carry out an experiment in which one of the two polarizations f_N, f_n is zero. In this case, the expression simplifies substantially. For $f_n = 0$,

$$\Delta E_0 = -f_N H \left\{ \left[1 - \frac{1}{(2I+1)(I+1)} \right] \mu_b - \mu_0 \right\} \quad (J = I + 1/2),$$
$$\Delta E_0 = -f_N H (\mu_b - \mu_0) \quad (J = I - 1/2). \qquad (29)$$

For $f_N = 0$,

$$\Delta E_0 = -\frac{1}{3} f_n H \left[\left(1 + \frac{2}{2I+1} \right) \mu_b - \mu_0 \right] \quad (J = I + 1/2),$$
$$\Delta E_0 = -\frac{1}{3} f_n H \left[\left(1 + \frac{1}{I} \right) \mu_0 - \mu_b \right] \quad (J = I - 1/2). \qquad (30)$$

The shift is measured from the energy of the state in the absence of both polarizations.

The shift ΔE_0 is extremely small: If we assume that μ_b and μ_0 differ by 1 nuclear magneton and that the field at the nucleus is $H = 10^6$ Oe, we find $\Delta E_0 \approx 3 \cdot 10^{-6}$ eV, which is four or five orders of magnitude less than the intrinsic width of the neutron resonances. It is thus clear that we could hope for successful measurements only for the nuclei of rare earth elements, with internal fields running to several million oersteds.

A series of studies of the magnetic moments of several compound states of rare earth nuclei has been carried out in the Neutron Physics Laboratory of the Joint Institute for Nuclear Research, Dubna.[85,86] The transmission of neutrons through foils of rare earth metals (Tb, Dy, Ho, and Er) was studied by a time-of-flight method in an IBR-30 fast-neutron pulsed reactor.[42] The nuclei of these rare earths were polarized by extreme cooling (≈ 30 mK) in a refrigerator using the dissolution of ^{3}He in ^{4}He. The internal magnetic fields at these nuclei were $(3-7) \cdot 10^6$ Oe. Under these conditions, the polarization of the nuclei within the domains ranged from 0.84 to 0.99. The polarization was destroyed by raising the target temperature to $0.5-1.5$ K.

Alternate measurements with polarized and unpolarized nuclei yielded time-of-flight spectra, in which the relative shifts of the resonances are described by expression (29). Figure 16 shows a representative spectrum, obtained in an experiment with dysprosium. Throughout all the measurements, some reference targets were kept in the beam continuously; the resonances of these targets were used as a time reference for the spectra and in order to monitor the operation of the apparatus.
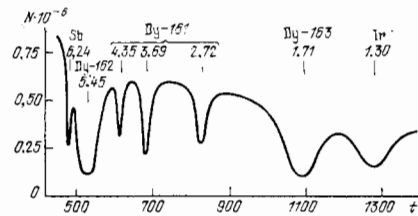

FIG. 16. Part of an experimental spectrum obtained in measurements over 6 h. N—number of counts per channel; t—the channel of the time analyzer. Shown at the top are the isotopic identification and the energy of the resonances, in electron volts. Sb and Ir are reference targets.

The shift of the resonance energy was determined by a computer-assisted least-squares fit of the spectra for the polarized nuclei to those for the unpolarized nuclei. The very small value of this shift required a high statistical accuracy of the spectra and also required many control experiments to evaluate possible secondary effects. Lengthy experiments (about 300 h of measurement time for each element) yielded the magnetic moments listed in Table III for the compound nuclear states. Shown in the same table are the values of $g = \mu_b/J$, where J is the spin of the resonance.

Analysis of Table III shows that the magnetic moments were not determined very accurately; the smallest error is $0.4\mu_N$. Furthermore, it would be difficult to expect any significant improvement in the accuracy in the near future, since even in these experiments the error corresponds to an extremely small shift of the resonance, by an amount equal to 10^{-4} of the intrinsic width of the resonance, $\Gamma \approx 0.1$ eV. It is also unlikely that there will be any significant increase in the numbers of levels and nuclei for which magnetic moments are measured, because of the requirement of strong fields at the nuclei and the presence of low-energy resonances. Nevertheless, the information gained in these experiments is sufficient to give us a general idea of the magnetic moments of the compound states of rare earth nuclei and to make a comparison with theoretical predictions of these moments.

Apparently the first theoretical paper to appear with predictions of the magnetic moments of compound

TABLE III. Experimental data on the magnetic moments of resonances.

Compound nucleus	E_0, eV	J	ΔE_0, 10^{-6} eV	μ_b, nuclear magneton	g
^{160}Tb	3.35	2	19 ± 9	-0.2 ± 1.0	-0.1 ± 0.5
	4.99	1	-20 ± 33	4.3 ± 3.7	4.3 ± 3.7
	11.1	2	31 ± 39	-1.7 ± 4.4	-0.8 ± 2.2
^{162}Dy	2.72	3	1.3 ± 8.9	-0.4 ± 0.7	-0.13 ± 0.23
	3.69	2	-16.1 ± 10.7	-1.8 ± 0.9	-0.90 ± 0.45
	4.35	2	11.4 ± 14.8	0.5 ± 1.2	0.25 ± 0.60
^{164}Dy	1.71	2	-28.3 ± 5.9	2.8 ± 0.5	1.40 ± 0.25
^{166}Ho	3.93	4	36 ± 12	1.8 ± 0.7	0.45 ± 0.17
	12.7	4	4 ± 30	3.9 ± 1.9	0.98 ± 0.47
^{168}Er	0.46	4	27 ± 7	0.9 ± 0.4	0.22 ± 0.10
	0.58	3	44 ± 16	1.8 ± 0.9	0.6 ± 0.3

states was that by Kuklin.[87] The theory derived there was based on the statistical model, and the results correspond to averages over many levels. Kuklin derived the following expression for the average g-factor for a "heated" nucleus with an excitation energy comparable to the neutron binding energy:

$$\bar{g} = \frac{\bar{\mu}}{\bar{I}} = \frac{J_p}{J_T},$$

where J_p and J_T are the proton and total moments of inertia of the nucleus. Assigning these moments of inertial their solid-state values, Kuklin[87] derived the estimate

$$\bar{g} = \frac{Z}{A}, \tag{31}$$

where Z and A are the charge and mass number of the given nucleus. Fluctuations around the average value are of a magnitude

$$\frac{\Delta g}{\bar{g}} = \sqrt{\frac{A-Z}{Z}}. \tag{32}$$

Bunatyan carried out a more detailed and more rigorous analysis, using the method of temperature Green's functions. In Ref. 88, using a semiclassical approximation for $\bar{g}$, he rederived the expression derived by Kuklin but found the fluctuations to be about half as large. In Ref. 89 Bunatyan carried out calculations for nuclei in the rare earth region without resorting to the semiclassical approximation. He showed that the semiclassical values in (31) are reached at nuclear excitation energies higher than the neutron binding energy. Numerical calculations carried out for rare earth nuclei yield $\bar{g} = 0.28$ (an average was taken over the five isotopes for which measurements were carried out). This value is slightly smaller than the ratio $Z/A \approx 0.4$ for the nuclei in the rare earth region. As for the fluctuations, it was noted that their size may depend on the pairing-correlation energy for neutrons (Δ_n) and that for protons (Δ_p). The result may be a slight increase in the dispersion of g.

Blokhin and Ignatyuk[90] analyzed the magnetic moments of excited nuclei on the basis of a statistical model for spherical and deformed nuclei. Their results were similar to those which we just saw.

Another, semimicroscopic, approach was taken by Voronov and Solov'ev.[91] The qualitative result which they derived shows that the magnetic moments of the compound states can be expected to be approximately the same as those of the nuclear ground states.

We have been discussing the theoretical predictions of the magnetic moments which may be compared with the experimental data. As the experimental data, we may use the g-factors for all the compound states as a single statistical ensemble, since in these theoretical predictions there are essentially no distinctions between nuclei which have similar values of A and similar deformations. It can be seen from Table III and Fig. 17 that the scatter in the values is much larger than the experimental errors. It is thus possible to distinguish the fluctuations resulting from the physical
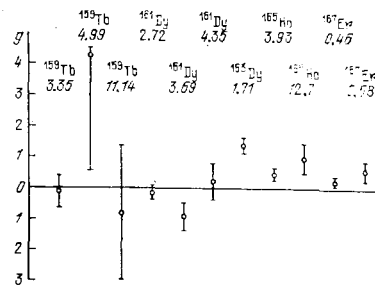

FIG. 17. The g-factors for the resonances studied. The isotopes and the energies of the resonances, in electron volts, are shown at the top.

nature of the phenomenon from those resulting from experimental errors. A statistical analysis[86] has yielded the following results:

$$\langle g \rangle = 0.34 \pm 0.22,$$
$$\Delta g = 0.51 \pm 0.20.$$

Comparing these results with the theoretical predictions discussed above, we see that both the average value of the gyromagnetic ratio and the size of its fluctuations agree with the predictions of the statistical theory. It is hardly worthwhile to attempt a more detailed comparison with the various studies, since the differences lie within the uncertainty in both the experimental and theoretical values. It may thus be concluded that the description of the magnetic moments of compound and nuclear states which emerges from the statistical model is valid and that this model thus finds support in yet another area.

b) Change in the rms charge radius of a nucleus upon the capture of a resonance neutron

The measurements of the magnetic moments of compound states which we just discussed made use of the effect of the hyperfine magnetic interaction on the position of a neutron resonance. We turn now to some experiments in which the electrostatic hyperfine interaction made it possible to detect the change in the rms charge radius of a nucleus upon the capture of a resonance neutron.

The isomer chemical shifts for low-lying excited nuclear states have been studied in detail by Mössbauer spectroscopy. Such shifts are observed in a comparison of γ transitions for a given nucleus in different chemical compounds, provided that the nucleus has different shapes in its ground and isomer states. The magnitude of this shift can be approximated by

$$\Delta E = \text{const} \cdot \Delta \rho_e(0) \, \Delta \langle r^2 \rangle.$$

It is proportional to the difference between the electron densities at the nucleus, $\Delta \rho_e(0)$, for the two chemical compounds, and it is proportional to the difference between the rms radii of the nucleus, $\Delta \langle r^2 \rangle$, in its excited and ground states. It can be seen from this expression that measurements of the isomer shift can yield the change in the rms radius of the nucleus upon

excitation if $\Delta\rho_e(0)$ is known from other experiments or calculations. Mössbauer spectroscopy can be used to study only the lowest-lying excited nuclear states. Ignatovich *et al.*[92] have raised the possibility of carrying out corresponding measurements for levels with excitation energies corresponding to the neutron binding energy in the nucleus. Their estimates showed that by very precisely determining the positions of a neutron resonance in different chemical compounds one could use the shift in the resonance energy to determine the change in $\langle r^2 \rangle$ upon neutron capture. This shift could be expected to be of the order of 10^{-4} eV; the feasibility of measuring such shifts was demonstrated by the measurements of the magnetic moments, which we just discussed. In experiments on chemical shift, however, there is the further difficulty that it is necessary to compare the resonance dips in the transmission spectra of neutrons for targets of different chemical compounds. The Doppler broadening of the resonance[93] which results from the vibrations of the crystal lattice differs from compound to compound and may give rise to an apparent shift of the same order of magnitude as the effect of interest.

Despite these difficulties, experiments were carried out in the Neutron Physics Laboratory of the JINR, and they revealed a change in the rms radius of the ^{238}U nucleus upon the capture of a resonance neutron.[94,95]

Let us examine the theoretical description of the chemical shift of neutron resonances. As mentioned earlier, this shift is an analog of the Mössbauer isomer shift. A comprehensive theory for this effect has been published in several places; for our discussion we will take the approach of Ref. 96.

The electrostatic interaction between a nucleus and an electron in an atom can be described by

$$U = -e^2 \int\int \frac{\rho_e(r_e)\,\rho_p(r_p)}{|r_e - r_p|}\, d\tau_e\, d\tau_p, \tag{33}$$

where $\rho_e(r_e)$ and $\rho_p(r_p)$ are the electron and proton densities, and the integrals are evaluated over the volume occupied by the electrons and protons. We then write the expansion

$$\frac{1}{|r_e - r_p|} = \sum_{l=0}^{\infty} \sum_{m=-l}^{l} \frac{2\pi}{2l+1} \left(\frac{r_<^l}{r_>^{l+1}} \right) Y_{lm}(\theta_p,\,\varphi_p)\, Y_{lm}(\theta_e,\,\varphi_e), \tag{34}$$

where the Y_{lm} are spherical harmonics, and $r_<$ and $r_>$ are the smaller and larger of the quantities $|r_e|$, $|r_p|$. Substituting (34) into (33), we find the electrostatic hyperfine interaction as a sum of multipoles of order l. The odd terms vanish, as can be seen from symmetry considerations. The $l=2$ term describes the quadrupole interaction and is of no interest here. The terms with $l \geqslant 4$ are small and can be discarded. We are thus left with the following expression for the electric monopole interaction, which is primarily responsible for the level shift:

$$U_0 = -e^2 \int\int \frac{\rho_e(r_e)\,\rho_p(r_p)}{r_>}\, d\tau_e\, d\tau_p. \tag{35}$$

The quantity U_0 is a measure of the difference between the energy states of the "bare" nucleus, i.e., that from
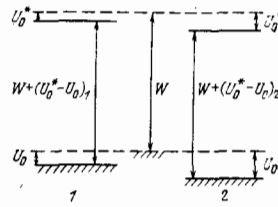

FIG. 18. The level shift resulting from the electrical interaction of a nucleus with the electron cloud. Dashed lines—ground and excited levels of the "bare" nucleus; 1, 2—levels in different chemical compounds.

which all the electrons have been stripped, and a nucleus with electron shells. This difference cannot be observed; all that is observable is the energy of a transition between levels, e.g., the energy of a γ ray or of a neutron. In turn, the energy shift suggests a comparison of transitions which differ in some way. The shift ΔE_0 can thus be written in the form

$$\Delta E_0 = (U_0^* - U_0)_1 - (U_0^* - U_0)_2. \tag{36}$$

The subscripts 1 and 2 designate different chemical compounds, while the asterisks refer to the excited nuclear state. The diagram in Fig. 18 illustrates expression (36). The dashed lines represent the ground and excited states of the "bare" nucleus, and W is the energy of the corresponding transition. It is easy to see that a difference between the transition energies in compounds 1 and 2 leads to (36). By substituting into (36) the values of U_0 from (35) for the ground and excited states of the nucleus in the two chemical compounds, we find an expression which, although quite accurate, is complicated and thus of little practical use. Accordingly, in research on isomer shifts it is customary to adopt several approximations, which simplify the resulting expression but which do not introduce a noticeable error, according to estimates. These assumptions can be written

$$\rho_e^*(r_e) = \rho_e(r_e), \tag{37a}$$

$$\rho_{p1}^*(r_p) = \rho_{p2}^*(r_p) = \rho_p^*(r_p), \tag{37b}$$

$$\rho_{p1}(r_p) = \rho_{p2}(r_p) = \rho_p(r_p). \tag{37c}$$

Relation (37a) means that the electron density does not change upon excitation of the nucleus; relations (37b) and (37c) mean that the charge density of the nucleus, in either its excited or ground state, does not depend on the particular chemical compound. Using (37a), (37b), and (37c) in (35) and (36), we find the expression

$$\Delta E_0 = -e^2 \int\int \frac{\Delta\rho_e(r_e)\,\Delta\rho_p(r_p)}{r_>}\, d\tau_e\, d\tau_p, \tag{38}$$

where

$$\Delta\rho_e(r_e) = \rho_e(r_e)_1 - \rho_e(r_e)_2,$$
$$\Delta\rho_p(r_p) = \rho_p^*(r_p) - \rho_p(r_p).$$

At this point it is convenient to switch to the electron density averaged over solid angle:

$$\rho_e'(r_e) = \frac{1}{4\pi} \int_\Omega \rho_e(r_e) \sin\theta\, d\theta\, d\varphi .$$

After some manipulations, we can write the shift as

$$\Delta E_0 = -4\pi e^2 \int \Delta \rho_p(\mathbf{r}_1)\, \mathscr{P}(\mathbf{r}_p)\, d\tau_p,$$

where

$$\mathscr{P}(\mathbf{r}_p) = \int_0^{r_p} \Delta \rho_e'(r_e) \left(\frac{1}{r_p} - \frac{1}{r_e} \right) r_e^2 \, dr_e.$$

The manipulations which follow involve a representation for the radial profile $\Delta \rho_e'(r_e)$ in the nucleus. For light nuclei, relativistic effects are unimportant for the behavior of the electrons; only s electrons, with their spherically symmetric distribution, contribute to the electron density at the nucleus; and the density itself is constant over the nucleus. In this case we have

$$\rho_e'(r_e) = \rho_e(r_e) = \rho_e(0),$$
$$\mathscr{P}(r_p) = -\frac{1}{6} r_p^2 \Delta \rho_e(0),$$

and for the resonance shift we find the simple expression

$$\Delta E_0 = \frac{2}{3}\pi e^2 Z \Delta \rho_e(0) \Delta \langle r_p^2 \rangle. \qquad (39)$$

This is the expression which is customarily used in a description of the isomer shift.

For heavy nuclei, the relativistic nature of the electron motion becomes appreciable, giving rise to a further increase in the electron density at the nucleus and causing a variation in $\rho_e(r_e)$ over the nucleus. In this case, expression (39) is replaced by a more complex expression, which incorporates higher-order moments of the nuclear charge distribution:

$$\Delta E_0 = \frac{2}{3}\pi e^2 Z \rho_e(0)[\Delta \langle r_p^2 \rangle - b_4 \Delta \langle r_p^4 \rangle + b_6 \Delta \langle r_p^6 \rangle - \ldots]. \qquad (40)$$

The chemical shift has been studied experimentally[94,95] for a resonance of ^{238}U (at 6.67 eV). The transmission of neutrons through targets of various chemical compounds of uranium was measured. The experiments were carried out by a time-of-flight method in the IBR-30 reactor operating in the booster mode. The baseline was about 60 m. A small computer was used to store the time-of-flight spectra of the neutrons and to monitor and control the experimental apparatus. The automated system made it possible to place each of three targets in the beam in turn, at intervals of 5 min. A total of five chemically different targets were used in these experiments, and the measurements were taken in various combinations.

The resonance shift for each pair of targets was found by a computer analysis of the spectra, which allowed for the effect of lattice vibrations on the shape of the resonance. This effect was determined on the basis of a series of special experiments and calculations.[95]

In order to go from ΔE_0 to the value of $\langle r_p^2 \rangle$, which is of interest, it is necessary to know the differences between the electron densities at the nucleus, $\Delta \rho_e(0)$, for all pairs of chemical compounds. These differences were derived from the model of effective valence-electron configurations, through the use of various experimental results.
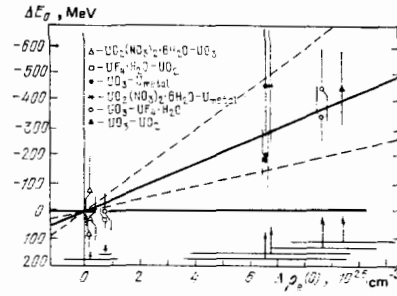

FIG. 19. The chemical shift of the resonance, ΔE_0, as a function of the difference between electron densities, $\Delta \rho_e(0)$, of the indicated pairs of chemical compounds.

Figure 19 summarizes the data, which show the dependence of the chemical shift of the resonance, ΔE_0, on $\Delta \rho_e(0)$. For each pair of targets the indicated error includes both the error of the measurements and the error in the correction for the broadening of the resonance by the vibrations of the crystal lattice. The horizontal line segments near the bottom of the figure illustrate the uncertainty in $\Delta \rho_e(0)$ for the corresponding pair. The solid line is drawn by the method of least squares through the experimental points and the origin; the dashed lines indicate the 95% confidence interval. The slope of the solid line, after a correction for the variation in $\rho_e(r_e)$ within the nucleus, yields the change in the rms charge radius of the ^{238}U nucleus upon the capture of a resonance neutron:

$$\Delta \langle r_p^2 \rangle = -(1.7^{+1.2}_{-0.8}) \quad F^2.$$

The indicated errors correspond to a 95% confidence interval. According to the data of Ref. 97, the rms radius of ^{238}U is $\langle r_p^2 \rangle = 34$ F^2; it is thus found that $\langle r_p^2 \rangle$ decreases by about 5% upon the capture of a neutron. Since the difference between the values of $\langle r_p^2 \rangle$ for the ^{238}U and ^{239}U ground states is only about 0.1 F^2, we may conclude that the observed decrease in $\langle r_p^2 \rangle$ is a consequence of the excitation of the nucleus by an energy equal to the binding energy of the neutron, $B_n = 4.8$ MeV.

Bunatyan[98] has derived estimates of the change in $\langle r_p^2 \rangle$ upon excitation of a nucleus. Taking a statistical approach, he showed that the rms radius decreases upon excitation to an energy of the order of the neutron binding energy, but the effect is about an order of magnitude smaller than that measured in the experiments just described.

Details of the observed decrease in $\langle r_p^2 \rangle$ cannot be determined from these experiments. One possible reason is a decrease in the deformation upon excitation. Calculations show that for the ^{238}U nucleus, whose deformation corresponds to the parameter $\beta = 0.25$, the rms radius decreases by 5% if the nucleus becomes more nearly spherical. Such a decrease would be difficult to expect, however, on the basis of all the experimental and theoretical data available. In summary, the first direct measurement of the change in the rms radius of a nucleus yielded an unexpected

result, which requires further study and theoretical interpretation.

5. PROPERTIES FOUND FOR FEW-NUCLEON SYSTEMS BY NEUTRON SPECTROSCOPY

The study of neutron-induced nuclear reactions of light nuclei has historically played a significant role in establishing the basic concepts of nucleon–nucleon interactions and in explaining the general features of these interactions. The group of lightest nuclei includes the proton, the deuteron, the triton, and the ^{3}He and ^{4}He nuclei. These nuclei are distinguished by their simple structure and the absence of nucleon-stable excited states. It is thus possible to take direct theoretical approaches in calculations for few-nucleon systems, both by using the many-body Schrödinger equation and by introducing nuclear wave functions in variational methods. The validity and usefulness of the various theories are tested in comparisons with such experimental data as the scattering lengths, the scattering phase shifts, and the magnitudes and energy dependence of the reaction cross sections. Most of these experimental data have been obtained by neutron spectrometry, primarily high-intensity spectrometry. Refinements of, and additions to, the experimental data and the development of theoretical approaches are being actively pursued at present.

a) Neutron scattering lengths

Phenomenologically, the interaction of slow s-wave neutrons with the lightest nuclei can be described [for each of the two spin states of the compound system $(J_\pm = 1 \pm 1/2)$] by two parameters: the scattering length a and the effective radius r_0. This circumstance was noted by Landau and Smorodinskiĭ[99] in 1944 and was used by Blatt (and also by Bethe, Schwinger, and others; see Ref. 100, for example) to develop a simple theoretical approach known as the effective-radius approximation. According to this approximation, the cross section for scattering in the channel with spin J is

$$\sigma_n(J) = 4\pi g_J \left[\left(-\frac{1}{a_J} + r_{0J}k^2 \right)^2 + k^2 \right]^{-1},\qquad (41)$$

where $k = \sqrt{2}\mu E/\hbar^2$ is the wave number of the neutron in the c.m. frame. At energies $E \leqslant 100$ eV, the terms with k and k^2 can be ignored, and the cross section becomes

$$\sigma_n = 4\pi(g_+a_+^2 + g_-a_-^2).\qquad (42)$$

For neutrons at thermal energies ($E \approx 0.025$ eV), coherent scattering is also measured. This type of scattering is described by the coherence length

$$a_{coh} = g_+a_+ + g_-a_-\qquad (43)$$

and the incoherent cross section

$$\sigma_{incoh} = 4\pi g_+ g_- (a_+ - a_-)^2.\qquad (44)$$

Only two of Eqs. (42)–(44) are independent. Since the cross section is a quadratic function of the scattering length, any pair of independent equations is satisfied by two sets of lengths. A polarization experiment is usually carried out to choose between these sets. The difference between the scattering lengths a_+ and a_- for few-nucleon systems is the most characteristic manifestation of the spin dependence of the neutron–nucleus interaction.

Among the primary sources of data on np scattering are Refs. 101 and 102. For nd scattering the results obtained in different studies, especially the results on the doublet length, remained severely at odds for a long time. A reconciliation was made possible after measurements of σ_n and a_{coh} by the Koester group[103] (Garching, FRG). They constructed a gravitational refractometer in order to determine a_{coh} by the method of specular neutron reflection. A circumstance aiding precise measurements of the critical reflection angle in this refractometer was the long distance (110 m) over which the neutron fell in the earth's gravitational field before it reached a liquid mirror of the test substance (D_2O in that case). The mirror was placed at various heights H; total reflection occurred only at a certain H^*. The length a_{coh} was determined from the expression $a_{coh} = (gm^2/2\pi N\hbar^2)H^*$.

As mentioned earlier, the values of a_{coh} and σ_n are not sufficient for an unambiguous determination of the scattering lengths. This problem was particularly acute for nd scattering, since different theoretical approaches led to mutually exclusive sets of scattering lengths. The correct set for nd scattering was determined by Shapiro's group[104] at the Neutron Physics Laboratory of the JINR, using the polarization method mentioned in Sec. 2. In addition to the polarized proton target (the beam polarizer), they constructed a dynamically polarized deuteron target. This experiment determined a set of scattering lengths with a predominant quartet length. In np scattering the ambiguity regarding sets of scattering lengths was resolved in experiments with ortho-hydrogen and para-hydrogen.

Figure 20 shows the most recent data on the nd system, which incorporate the polarization results of Ref. 104. This figure demonstrates the relationships between the quartet scattering length a_4 and the doublet scattering length a_2 corresponding to various measured cross sections: the coherent cross section σ_{coh}, the incoherent cross section σ_{incoh}, the total cross section for the free atom, σ_n, and the total cross section for ortho-deuterium molecules. It should be noted that,
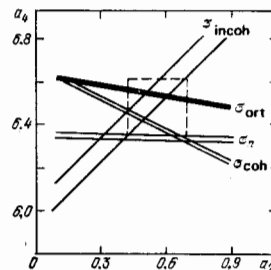

FIG. 20. Relationships between the a_2 and a_4 from various experiments.

TABLE IV. Experimental parameters of np and nd scattering.

System	σ_t, b	a_{coh}, F	Scattering lengths, F		Effective radius, F	
			a_+	a_-	r_+	r_-
np	20.491 (14)	3.741 (1)	5.424 (4)	−23.748 (10)	1.759 (5)	2.75 (5)
nd	3.390 (12)	6.672 (7)	6.35 (2)	0.65 (4)	1.85 ( )	—

in view of the high accuracy of each experimental result, the agreement is poor. Nevertheless, the set of scattering lengths based on the data on Ref. 103 and Eqs. (42) and (43) found general acceptance. This set is shown in Table IV along with the results of these studies for np scattering as of the most recent compilation.[105] Here a_+ and a_- correspond to the triplet and singlet states in the case of the np system or to the quartet and doublet states in the case of the nd system. The numbers in parentheses are the experimental errors in the last significant figures.

These experimental results, obtained by neutron spectroscopy, are of fundamental importance in nuclear physics. They are reference data which are used to test both new models for nucleon–nucleon interactions and any theory for few-nucleon systems. The large difference between the neutron–neutron scattering length $[a_{nn} = -16.6(5)$ F$]$ and the neutron–proton scattering length in the singlet state $[a_{np} = -23.75(1)$ F$]$ definitely indicates that the charge invariance of nuclear forces is not an absolutely rigorous law of nature. A difference at this level corresponds to an np interaction potential which is about 3% higher than the nn potential. This difference has been ascribed to a difference between the masses of the charged and uncharged mesons, since only neutral mesons participate in the exchange interaction between identical nucleons, while charged π and ρ mesons participate in the np case.

Of particular interest for theories of three-nucleon systems is the doublet nd scattering length, which is the parameter most sensitive to the detailed properties of the nuclear forces. The present state of these theories is reviewed by Kharchenko.[107] The experimental error in this scattering length is presently about 10%, and in future it may begin to become possible to compare the various theories. In the approach worked out at Dubna by Efimov,[106] for example, the doublet length a_2 is a parameter which is used to take into account the many-body, essentially quark, nature of the short-range three-nucleon interaction.

For the four-nucleon system, the next one up on the complexity scale, both experiment and theory lagged behind the progress on the np and nd systems for a long time. Here we are talking about an interaction of a neutron with tritium and with helium-3. Experimental difficulties result from the radioactivity of the target in the case of tritium and the very large cross section (5337 b) of the competing (n,p) reaction in the case of helium-3. On the theoretical side, although the rigorous Faddeev–Yakubovskiǐ equations had been written, the existing computers were not powerful enough to solve them.
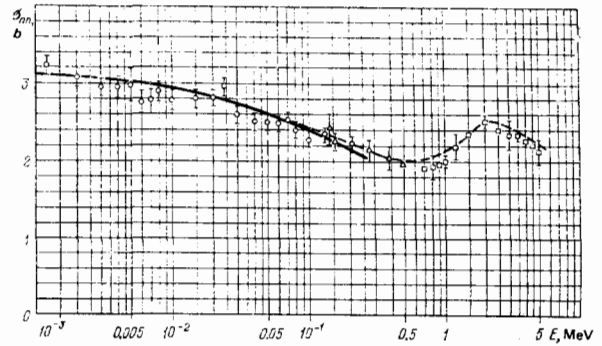

FIG. 21. Effective cross section for neutron scattering by helium-3, as a function of the neutron energy.[110]

Progress was reached in the late 1970's, essentially simultaneously in the experimental and theoretical areas. The cross sections σ_n(^{3}He) at $E \leqslant 1$ eV were measured with thin gaseous samples (up to 30 torr; a JINR experiment[108]), and the coherence length a_{coh} was measured with a new instrument: a neutron interferometer (an ILL experiment[109]). It later became possible to determine the cross sections for higher energies, up to 200 keV. These cross sections are shown in Fig. 21 in Ref. 110. These data provided, over a broad energy range, an independent determination of the n^{3}He scattering lengths in the zeroth approximation in the effective radius: Re$a_s = 6.53 \pm 0.32$ F, Re$a_t = 3.62 \pm 0.15$ F (Ref. 110). In turn, the joint use of a_{coh} (Ref. 109) and σ_n($\leqslant 1$ eV) (Ref. 108) in accordance with Eqs. (42) and (43) led to the results[109] 6.6 ± 1.1 and 3.55 ± 0.38 for the singlet and triplet scattering lengths, respectively.

For nT scattering, the experimental data (on σ_n and σ_{coh}) remained inconsistent for a long time and did not provide values for the scattering lengths. In 1980, measurements of the total nT cross sections were completed at Los Alamos.[111] These measurements were based on the transmission of gaseous samples and were carried out by a time-of-flight method over the energy range 60 keV–80 MeV. The samples were at pressures up to 171.4 atm (corresponding to an activity of $2 \cdot 10^5$ Ci). The scattering cross section extrapolated to zero energy turned out to be 1.70 ± 0.06 b. Because of the large error in the coherence length, the latter was not used in the analysis; the nT scattering lengths were obtained on the basis of theoretical arguments regarding the length ratio a_+/a_- (which was assumed to be 0.92 ± 0.04). The results presently available on the four-nucleon system are shown in Table V.

The values shown in Table V are taken from Refs. 110 and 111. The theoretical values[107] were found by

TABLE V. nT and n^{3}He scattering lengths.

System		Re a_s, F	Im a_s, F	Re a_t, F	Im a_t, F
nT	(expt)	3.91 (12)	—	3.60 (10)	—
nT	(theo)	3.77 (3.89)	—	3.13 (3.22)	—
n^{3}He	(expt)	6.53 (32)	4.45 (1)	3.62 (15)	$1.7 (8) \cdot 10^{-8}$
n^{3}He	(theo)	8.05 (9.42)	—	3.08 (3.15)	—

solving the Faddeev–Yakubovskiĭ equations with the simplest separable NN potentials; the Coulomb interaction was ignored. The numbers shown without parentheses correspond to calculations with a Yukawa form factor, while the numbers in parentheses correspond to calculations with an exponential form factor. According to the theory, the interaction of a slow neutron with a triton reduces primarily to an effective repulsion at distances of the order of the size of the triton; the situation is similar to the scattering of a neutron by a deuteron in the quartet spin states. In the scattering of the neutron by the ^{3}He nucleus in the singlet state, however, the attractive nature of the interaction gives rise to an excited bound state with spin and parity 0^+ (more on this below).

Comparison of the experimental and theoretical results in Table V leads to the conclusion that the agreement is even better than qualitative. The discrepancies which remain point to the need for a further refinement of the theoretical methods used to derive the properties of the four-nucleon systems; at present, the theoretical methods are not as accurate as the methods available for the three-nucleon systems.

b) First excited level of the ^{4}He nucleus

Helium-4 is the first nucleus in the periodic table which has excited levels. The possible existence of such levels was discussed theoretically as early as 1936 by Feenberg,[112] who reached the conclusion that such levels do exist if certain assumptions are made regarding the nuclear forces. Convincing experimental proof came 20 years later with the help of a moderation-time spectrometer[113] at the Lebedev Physics Institute, Moscow; these measurements revealed a pronounced deviation of the ^{3}He(n, p) cross section from the $1/v$ law and showed that the reaction goes through a single spin channel. These results were ascribed to the existence of an excited level with an energy of about 20 MeV and a spin $J^\pi = 0^+$. This conclusion was confirmed by a polarization experiment.[114] The details of the deviation of the cross section $\sigma_{np}(^3\text{He})$ from the $1/v$ law were recently studied[115] up to neutron energies of about 150 keV (Fig. 22), through the use of a time-of-flight method.
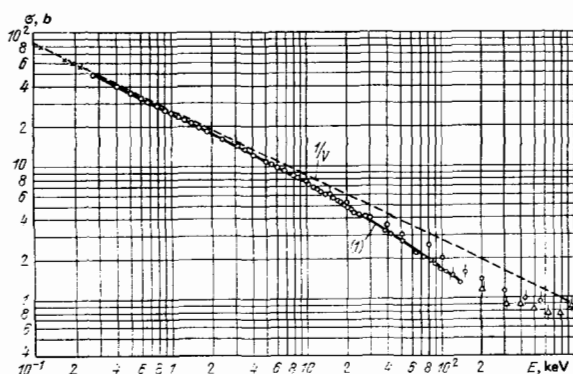

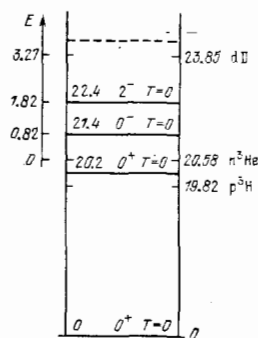FIG. 22. Effective cross section for the reaction ^{3}He(n, p), as a function of the neutron energy.[115]

FIG. 23. Scheme of the first few levels of the ^{4}He nucleus. Right—scale of the thresholds for the various decay channels; left—kinetic energy in the c. m. frame of the neutron and the ^{3}He nucleus.

The first excited level of ^{4}He has also been manifested in many other reactions, including the reaction ^{3}He(d, p)^{4}He, the elastic scattering T(p, p)T, and the inelastic reactions ^{4}He(e, e')^{4}He and ^{4}He(α, α'). Among the studies of the latter reaction we wish to call attention to one of the new studies of the inelastic scattering of α particles by helium-4, carried out by Baumgartner et al.[116] An R-matrix analysis of the results of that experiment confirmed, in particular, the set of n^{3}He scattering lengths discussed in the preceding section. The quantitative characteristics, however, especially the reduced widths of the first excited level of ^{4}He, remained undetermined for a long time. To some extent the difficulty resulted from the special position of the 0^+ level, between the thresholds for two channels (Fig. 23). Threshold effects arise, and the reaction cross section cannot be described by the simple formula in (4). It becomes necessary to use more rigorous expressions, e.g., the one-level approximation of R-matrix theory:

$$\sigma_{np} = \frac{\pi g}{\lambda^2} \frac{\Gamma_n \Gamma_p}{|E_\lambda + \Delta_\lambda(E) - E|^2 + (\Gamma^2/4)}$$

This expression contains some quantities which do not appear in (4): the characteristic energy E_λ and the level shift Δ_λ, which are determined by the boundary conditions of the problem; the reduced widths; and the shift functions, which were determined in Ref. 15. If we formally identify the term $E_\lambda + \Delta_\lambda$ with E_0 in (4), we find that the effective resonance energy E_0 becomes a function of the parameters E_λ, γ_n^2, and γ_p^2 and of the energy E. The net result is that the energy dependence of the reaction cross section, $\sigma_{np}(E)$ can be described equally well by various combinations of these parameters. For a set of experiments of different types, e.g., scattering and absorption, the uncertainty is reduced, but it is not completely eliminated. For example, according to Ref. 115 the two sets of parameters ($E_\lambda = 20.36$ MeV, $\gamma_n^2 = \gamma_p^2 = 3.4$ MeV) and (20.32 MeV, 10 MeV) lead to cross sections differing by less than 1% and consequently correspond to a single smooth curve in Fig. 22. Manifestations of the broad 0^+ level as narrow peaks (0.3–0.5 MeV) in several experiments with charged particles[116] are a consequence of these threshold effects.

The theory on the subject has not yet furnished a satisfactory explanation for the properties of the first excited level of helium-4. According to the shell model, the lowest-lying excited level with a spin $J = 0$ has a negative parity, in contradiction of experiment. When the theoretical parameters are fitted to the experimental characteristics of this level, the model fails to reproduce all the rest of the spectrum of excited levels of ^{4}He (Ref. 117). In an approximate solution of the Faddeev–Yakubovskiĭ equations without Coulomb forces, a 0* level arises (as mentioned above) as a second stationary set of the ^{4}He nucleus. Other theoretical approaches, e.g., the k-harmonic method and the various versions of the cluster model, have also failed to describe the properties of the 0* level of ^{4}He. The first excited level of helium-4 remains a subject for present and future research.

c) Radiative capture of neutrons by the lightest nuclei

The study of this reaction began at almost the same time at which the neutron was discovered. As early as 1935, Fermi drew attention to the magnetic nature of the γ emission in np capture and derived an expression which would be written in modern notation as

$$\sigma_{n\gamma}(^1 / l) \cdots 2\pi\alpha \frac{c}{v_n} (\mu_p - \mu_n)^2 \left(\frac{B_n}{Mc^2} \right)^{5/2} (\gamma^{-1} - a_s)^2; \quad (45)$$

here μ_p and μ_n are the magnetic moments of the proton and neutron, in units of the nuclear magneton; $\alpha = 1/137$, c is the speed of light; v_n is the neutron velocity; B_n is the binding energy of the deuteron; $\gamma = \sqrt{MB_n}/\hbar$ is the reciprocal of the effective size of the deuteron; and a_s is the singlet np scattering length. This expression is valid under the assumption that the deuteron ground state is a pure S state and that the entire interaction is generated exclusively by one-particle magnetic moments. The deuteron has a D-state admixture, on the other hand, and the exchange interaction between nucleons in the nucleus gives rise to additional (exchange) meson currents.

Nuclei more complex than the deuteron contain identical particles, and this situation gives rise to a small component of the S′ state of mixed symmetry in the wave function of the nucleus. In the case of the triton, for example, this state is antisymmetric with respect to the interchange of the coordinates of the neutrons and symmetric with respect to the spins. A further restriction is imposed on the cross sections $\sigma_{n\gamma}$ by the circumstance that M1 transitions can occur only between states for which the spin wave functions are of identical symmetry. The corresponding expressions, which are analogous to (45) for ^{2}H and ^{3}He targets, are given, for example, in Ref. 119. Zero cross sections are expected for ^{3}H and ^{4}He targets, since ground states of the ^{4}H and ^{5}He product nuclei do not exist. Neutron capture is possible, however, at energies sufficient to form nucleon-unstable states of these nuclei.

Interesting information has now been obtained in neutron physics regarding the radiative capture of neutrons by the lightest nuclei. Various experimental methods have been used to determine $\sigma_{n\gamma}$. A direct method is to measure the yield of γ rays from the (n,γ) reaction in which a nuetron beam passes through collimators and strikes a sample, and the γ rays which are produced in the reaction are detected by a detector making an angle θ with the direction of the neutron beam.

For a thin sample ($n\sigma \ll 1$) the number of "useful" detector counts N_γ is related to the differential cross section $\sigma_\gamma(\theta)$ by

$$N_\gamma = n\sigma_\gamma(0) \cdot \Pi(E_n) \cdot \varepsilon_\gamma \Delta\Omega, \quad (46)$$

where $\Pi(E_n)$ is the number of neutrons of energy E_n which are incident on the sample, ε_γ is the capture efficiency, $\Delta\Omega$ is the solid angle subtended by the detector, and n is the thickness of the sample (in nuclei per square centimeter). Absolute direct measurements require an independent determination of the factor $\Pi(E_n)\varepsilon_\gamma$—usually a difficult problem. In relative measurements, this factor is eliminated by means of a special experiment with a standard sample for which the cross section $\sigma_\gamma(\theta)$ is well known. Some of the results which we will discuss here were obtained in direct measurements of this sort, through the use of scintillation detectors with crystals and through the use of Ge(Li) semiconductor detectors. Figure 24 shows a representative γ spectrum obtained in Ref. 120 in a study of the reaction D(n,γ); a Ge(Li) detector was used. Difficulties arise in the study of this reaction and (especially) the reaction ^{3}He(n,γ) because the cross sections are small, and it is accordingly necessary to increase the transmission of the apparatus and to suppress carefully all other processes which might complicate the experiment. In several cases, the cross sections $\sigma_{n\gamma}$ have been determined by indirect methods for the lightest nuclei, by measuring the neutron lifetime in the medium, τ, and the diffusion length L. These measurements are based on neutron diffusion theory, according to which τ and L are related to the cross section $\sigma_{n\gamma}$ by

$$\tau = \frac{1}{N\sigma_{n\gamma}}, \quad L^2 = \frac{\lambda_{tr}}{3N\sigma_{n\gamma}}. \quad (47)$$
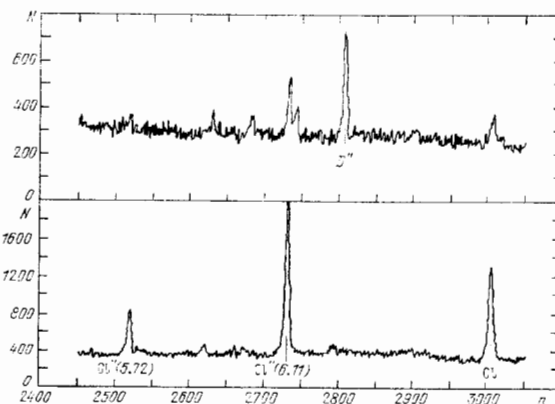

FIG. 24. Experimental spectrum of γ rays from the reaction D(n,γ), with the line D″ corresponding to capture by a deuteron (at the top) and the line Cl″, corresponding to capture by chlorine (at the bottom, calibration).[120]

TABLE VI. Cross sections for radiative capture of thermal neutrons by the lightest nuclei.*

Target nucleus	^{1}H	^{2}H	^{3}H	^{3}He	^{4}He
σ_{expt}, mb σ_{theo}, mb	332.6 (7) 303 (4)**	0.476 (20) 0.52 (5)	— 0	0.027—0.060 0.038 (20)	≤50 0

*According to the data from the studies analyzied in Ref. 119.
**Theoretical value ignoring meson exchange.

FIG. 25. Cross section for the radiative capture of neutrons by the ^{3}He nucleus, as a function of the neutron energy.[123]

Here N is the number density of nuclei in the medium, and λ_{tr} is the transport length.

In Table VI, which shows the data presently available, it is clear that as we go to the deuteron and then to the ^{3}He nucleus the cross section decreases sharply because of the selection rule regarding the symmetry of the wave functions of few-nucleon nuclei with respect to the interchange of identical nucleons.

The experimental value of $\sigma_{n\gamma}(^1$H) is 10% larger than the value found by the conventional theoretical approach using (45). Riska and Brown[121] introduced exchange currents in a consideration of the D state in the deuteron and achieved agreement with experiment. This fact is presently regarded as one of the important pieces of evidence for the mechanism of one-pion exchange between nucleons in a nucleus. Expression (45) corresponds to the singlet cross section, $\sigma_{n\gamma,s}$. The D-state admixture also gives rise to a triplet cross section $\sigma_{n\gamma,t}$. The latter cross section, however, is very small: $\sigma_{n\gamma,t}/\sigma_{n\gamma,s} \approx 10^{-4}$ according to measurements with polarized neutrons.[118]

The experimental error in the cross section $\sigma_{n\gamma}(^2$H) is about 5% and much larger than the error in $\sigma_{n\gamma}(^1$H). The uncertainty in the theoretical prediction[122] in this case is 10%. This prediction was generated from a microscopic theory for few-nucleon systems which uses separable nucleon potentials and which incorporates meson effects. Comparison with experiment seems to reveal evidence of one-pion exchange again in this case, since the contribution of exchange currents to the theoretical value is about 0.2 mb.

Finally, there is much uncertainty in the data on $\sigma_{n\gamma}(^3$He). Two experimental results have been obtained for thermal neutrons: 27 ± 9 μb (Ref. 123) and 60 ± 12 μb (Ref. 124). A theory incorporating only meson effects predicts a value[125] 38 ± 20 μb. On the other hand, it is also possible to explain the cross section $\sigma_{n\gamma}(^3$He) by considering S' states of the nuclei and ignoring exchange currents. This approach leads to an experimental estimate $0.05\% < P_{4He}(S') < 0.5\%$ for the component of mixed symmetry in the ^{4}He wave function. There is accordingly an urgent need for more accurate measurements of $\sigma_{n\gamma}(^3$He) and for more accurate calculations of this cross section.

In addition to the measurements of $\sigma_{n\gamma}(^3$He) at thermal energies, measurements have also been carried out in the range 1–70 keV (Ref. 123). The neutron flux densities fall off at these energies, but results have been obtained (Fig. 25) through the use of cryogenic
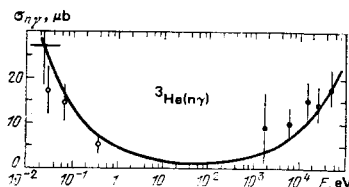
techniques in fabricating a target of liquid ^{3}He and through the use of the pulsed beam of the IBR-30 reactor. The energy dependence of the cross section indicated by the curve can be explained quite simply: At low energies, the decrease in the cross section with increasing energy obeys the $1/v$ law for s-wave neutrons. At high energies the cross section increases in accordance with the $\sqrt{E}$ dependence expected for p-wave neutrons.

6. CONCLUSION

We have examined several recent advances in high-intensity neutron spectrometry—advances which have yielded the first information from some new characteristics of highly excited nuclear states, new data on few-nucleon nuclear systems, and further information on the special class of nuclear reactions which involve a compound-nucleus step. Apparently a general result of this research is the conclusion that the new characteristics of the compound nuclei are described well in a first approximation by the modern statistical theory of the nucleus. Perhaps the only unexpected result has emerged from a study of the behavior of the rms radius of the deformed uranium nucleus. The effect is so large that—if it is confirmed by further measurements—it may force us to reexamine the fission of heavy nuclei.

The number of physical problems which arise from research by high-intensity neutron spectrometry, however, will continue to increase in the near future, and these questions will become more interesting. We might include here the search for and study of the ^{7}Be(n, 2α) reaction with the goal of detecting parity-nonconserving nuclear forces. The program for such research was examined in detail by Andreev some time ago.[126] Special experiments will apparently be carried out to search for the (n, ^{8}Be) reaction. Study of this reaction might shed light on the mechanism for the emission by a compound nucleus of such a weakly bound particle as ^{8}Be. Would it perhaps be more convenient to interpret this process as a very asymmetric fission?

Of decisive importance for progress on these questions and many others will be the successful implementation of high-intensity pulsed neutron sources, which are presently being adopted in neutron experiments. Examples are the IBR-2 pulsed reactor, proton accelerators with energies of about 1 GeV, and other high-current charged-particle accelerators.

We wish to thank I. M. Frank for reading the manuscript and for offering several useful comments.

[1]J. Chadwick, Nature **129**, 312 (1932).

[2]D. Iwanenko, Nature **129**, 798 (1932).

[3]W. Heisenberg, Z. Phys. **77**, 1 (1932).

[4]E. Fermi, Nature **133**, 757 (1934).

[5]P. B. Moon and R. Tillman, Proc. R. Soc. **153**, 421 (1936).

[6]N. Bohr, Nature **137**, 344 (1936).

[7]O. Hahn and Q. Strassmann, Naturwissenschaften **27**, 11 (1939).

[8]Ya. B. Zel'dovich and Yu. B. Khariton, Zh. Eksp. Teor. Fiz. **10**, 477 (1940).

[9]E. Amaldi, in: Handbuch der Physik, Vol. 38/2/Hrsg. (ed. S. Flugge), Springer-Verlag, Berlin, 1959.

[10]M. B. Fedorov, Spektrometriya neĭtronov srednikh énergiĭ (Spectrometry of Intermediate-Energy Neutrons), Naukova dumka, Kiev, 1979.

[11]R. E. Chrien and W. R. Kane (editors), Neutron Capture Gamma-Ray Spectroscopy, Plenum, New York, 1979.

[12]Yu. G. Abov and P. A. Krupchitskiĭ, Usp. Fiz. Nauk **118**, 141 (1976) [Sov. Phys. Usp. **19**, 75 (1976)].

[13]A. Michaudon, in: Nuclear Fission Neutron Induced Fission Cross Sections, Pergamon, New York, 1981.

[14]R. E. Chrien, Phys. Rep. **64**, 337 (1980).

[15]A. M. Lane and R. G. Thomas, Theory of Nuclear Reactions at Low Energies (Russ. Transl. IL, Moscow, 1960).

[16]G. Breit and E. P. Wigner, Phys. Rev. **49**, 519, 642 (1936).

[17]S. F. Mughabghab and D. I. Garber, Neutron Cross Sections, BNL-325, third edition, 1973.

[18]I. I. Gurevich and M. I. Pevsner, Nucl. Phys. **2**, 575 (1957).

[19]E. P. Wigner, in: Gatlinburg Conference on Neutron Physics, ORNL Report 2309, 1957, p. 59.

[20]H. Liou et al., Phys. Rev. **C5**, 974 (1972).

[21]T. A. Brody, J. Flores, J. B. French, et al., Rev. Mod. Phys. **53**, 385 (1981).

[22]C. E. Porter and R. G. Thomas, Phys. Rev. **104**, 483 (1956).

[23]D. F. Zaretskiĭ, and V. I. Sirotkin, Yad. Fiz. **27**, 1534 (1978) [Sov. J. Nucl. Phys. **27**, 808 (1978)].

[24]V. I. Bondarenko and M. G. Urin, in: Neĭtronnaya fizika: Materialy 5-ĭ Vsesoyuznoĭ konferentsii (Neutron Physics. Proceedings of the Fifth All-Union Conference), TsNIIatominform, Moscow, Vol. 1, 1980, p. 105.

[25]Kh. Maletski, L. B. Pikel'ner, I. M. Salametin, and É. I. Sharapov, Yad. Fiz. **13**, 240 (1971) [Sov. J. Nucl. Phys. **13**, 133 (1971)].

[26]J. M. Blatt and V. F. Weisskopf, Theoretical Nuclear Physics, Wiley, New York, 1952 (Russ. transl. IL, Moscow, 1954).

[27]D. J. Hughes, R. L. Zimmerman, and R. E. Chrien, Phys. Rev. Lett. **1**, 461 (1958).

[28]V. N. Kononov, in: Mezhdunarodnaya shkola po neĭtronnoĭ fizike (International School on Neutron Physics), Dubna, OIYaI DZ-11787, 1978, p. 415.

[29]H. H. Barschall, Phys. Rev. **86**, 431 (1952).

[30]H. Feshbach, C. E. Porter, and V. F. Weisskopf, Phys. Rev. **96**, 448 (1954).

[31]P. E. Nemirovskiĭ, Sovremennye modeli atomnogo yadra (modern Nuclear Models), Atomizdat, Moscow, 1960.

[32]B. Block and H. Feshbach, Ann. Phys. (N. Y.) **23**, 47 (1963).

[33]V. P. Alfimenkov et al., Nucl. Phys. **A376**, 229 (1982).

[34]U. Fasoli et al., Nucl. Phys. **A311**, 368 (1978).

[35]J. Harvey (editor), Experimental Neutron Resonance Spectroscopy, Academic, New York, 1970.

[36]F. W. K. Firk, Nucl. Instrum. Methods **162**, 539 (1979).

[37]V. F. Gerasimov, V. F. Lepnikov, M. I. Pevzner, and N. A. Chernoplekov, in: Neĭtronnaya fizika (Neutron Phys-ics), Vol. 2, Naukova dumka, Kiev, P. 201 (1972); R. M. Voronkov et al., At. Energ. **26**, 348 (1969).

[38]A. Bensussam and J. M. Salome, Nucl. Instrum. Methods **155**, 11 (1978).

[39]J. A. Harvey, in: II Mezhdunarodnaya shkola po neĭtronnoĭ fizike (Second International School on Neutron Physics), Dubna, OIYaI DZ-7991, 1974, p. 157; N. C. Peiring and T. A. Lewis, IEEE Trans. Nucl. Sic. **NS-16**, 31 (1969).

[40]J. E. Lynn, Contemp. Phys. **21**, 483 (1980).

[41]G. F. Auchampaugh, in: Nuclear Cross Sections for Technology: Proceedings of the International Conference (ed. J. L. Fowler and C. H. Johnson), Knoxville, 1979.

[42]I. M. Frank, Fiz. Elem. Chastits At. Yadra. **2**, 807 (1972).

[43]N. K. Abrosimov, G. Z. Borukhovich, et al., in: Neĭtronnaya fizika: Materialy 3-ĭ Vsesoyuznoĭ konferentsii, Kiev, 1975 (Neutron Physics. Proceedings of the Third All-Union Conference, Kiev, 1975), Part 6, TsNIIatominform, Moscow, 1976, p. 221.

[44]V. D. Anan'ev, D. I. Blokhintsev, et al., Prib. Tekh. Eksp. No. 5, 17 (1977).

[45]L. E. Lazareva, E. L. Feĭnberg, and F. L. Shapiro, Zh. Eksp. Teor. Fiz. **29**, 381 (1955) [Sov. Phys. JETP **2**, 351 (1956)].

[46]F. L. Shapiro, in: Tr. FIAN SSSR (Proceedings of the P. N. Lebedev Physics Institute, Moscow), Vol. 24, 1964, p. 3.

[47]R. E. Slovacek, R. C. Black, et al., Nucl. Sci. Eng. **62**, 455 (1977).

[48]D. D. Simpson and L. G. Miller, Nucl. Instrum. Methods **61**, 245 (1968).

[49]R. C. Greenwood and R. E. Chrien, Nucl. Instrum. Methods **138**, 125 (1976).

[50]V. P. Vertebnyĭ, A. L. Kirilyuk, et al., Cited in Ref. 43, Part 3, p. 151; A. V. Murzin, A. F. Rudak, and V. A. Libman, Cited in Ref. 24, Part 2, p. 257.

[51]Yu. G. Abov, A. D. Gul'ko, and P. A. Krupchitskiĭ, Polyarizovannye medlennye neĭtrony (Polarized Slow Neutrons), Atomizdat, Moscow, 1966.

[52]F. L. Shapiro, in: Nuclear Structure Study with Neutrons, North-Holland, Amsterdam, 1966, p. 223; Yu. V. Taran and F. L. Shapiro, Zh. Eksp. Teor. Fiz. **44**, 2185 (1963) [Sov. Phys. JETP **17**, 1467 (1963)].

[53]V. P. Alfimenkov, L. B. Pikel'ner, and É. I. Sharapov, Fiz. Elem. Chastits At. Yadra. **11**, 411 (1980) [Sov. J. Part. Nucl. **11**, 154 (1980)].

[54]J. A. Harvey and N. W. Hill, Nucl. Instrum. Methods **162**, 507 (1979).

[55]Ts. Vylov, B. P. Osipenko, and V. M. Chumin, Fiz. Elem. Chastits At. Yadra. **9**, 1350 (1978) [Sov. J. Part. Nucl. **9**, 530 (1978)].

[56]Yu. Andzheevski et al., Yad. Fiz. **32**, 1496 (1980) [Sov. J. Nucl. Phys. **32**, 774 (1980)].

[57]G. V. Muradyan, Cited in Ref. 24, Vol. 2, p. 94.

[58]R. D. Macfarlane and I. Almodovar, Phys. Rev. **127**, 1665 (1962).

[59]E. Cheifetz, I. Gilat, A. I. Yavin, and S. G. Cohen, Phys. Lett. **1**, 289 (1962).

[60]V. N. Andreev and S. M. Sirotkin, Yad. Fiz. **1**, 252 (1965) [Sov. J. Nucl. Phys. **1**, 177 (1965)].

[61]J. Kvitek and Yu. P. Popov, Phys. Lett. **22**, 186 (1966).

[62]Yu. P. Popov, Fiz. Elem. Chastits At. Yadra. **2**, 925 (1972) [Sov. J. Part. Nucl. **2**, 69 (1972)].

[63]A. Antonov, N. Balabanov, Yu. M. Gledenov, Pak Hong Chol, and Yu. P. Popov, Yad. Fiz. **27**, 18 (1978) [Sov. J. Nucl. Phys. **27**, 9 (1978)].

[64]S. G. Kadmenskiĭ and V. I. Furman, Fiz. Elem. Chastits At. Yadra. **6**, 469 (1975) [Sov. J. Part. Nucl. **6**, 189 (1975)].

[65]V. P. Vertebnyĭ, V. A. Vtyurin, V. A. Dolgov, A. L. Kirilyuk, Yu. P. Popov, and A. F. Fedorova, Report RZ-11392 Joint Institute for Nuclear Research, Dubna, 1978.

[66]I. M. Frank, in: Nuclear Structure Study with Neutrons (ed. J. Ero and J. Szucz), Budapest, 1974, p. 17.

[67]N. P. Balabanov, Yu. M. Gledenov, Pak Hong Chol, Yu. P. Popov, and V. G. Semenov, Nucl. Phys. **261**, 35 (1976).

[68]V. G. Solov'ev, Yad. Fiz. **13**, 48 (1971) [Sov. J. Nucl. Phys. **13**, 27 (1971)].

[69]Yu. Andzheevski, F. Bechvarzh, Vo Kim Tkhan', V. A. Vtyurin, and Yu. P. Popov, Report RZ-81-144, Joint Institute for Nuclear Research, Dubna, 1981.

[70]A. Emsallem, These., University Lyon, 1979.

[71]M. Asghar, A. Emsallem, R. Chery, C. Wagemans, P. D'Hondt, and A. J. Deruytter, Nucl. Phys. **A259**, 429 (1976).

[72]C. Wagemans, E. Allaert, A. DeClerq, P. D'Hondt, A. Deruytter, G. Barreau, and A. Emsallem, Nucl. Phys. **A362**, 1 (1981).

[73]N. S. Oakey and R. D. Macfarlane, Phys. Lett. **B26**, 662 (1968).

[74]W. Furman, K. Niedzwiedziuk, Yu. P. Popov, R. Rumi, V. Salatsky, V. Tishin, and P. Winiwarter, Phys. Lett. **B44**, 465 (1973).

[75]K. E. G. Lobner, Phys. Lett. **B26**, 369 (1968).

[76]L. Aldea and H. Seyfarth, in: Neutron Capture Gamma-Ray Spectroscopy (ed. R. Chrien and W. Kane), Plenum, New York, 1979, p. 529.

[77]Yu. Andzheevski, Vo Kim Tkhan', V. A. Vtyurin, and Yu. P. Popov, Report RZ-81-433, Joint Institute for Nuclear Research, Dubna, 1981.

[78]J. Kopecki, Cited in Ref. 76, p. 665.

[79]C. M. McCullagh and R. E. Chrien, Cited in Ref. 76, p. 687.

[80]Yu. P. Popov, Preprint R4-10805, Joint Institute for Nuclear Research, Dubna, 1977.

[81]S. G. Kadmenskii, V. P. Markushev, and V. I. Furman, Yad. Fiz. **31**, 1175 (1980) [Sov. J. Nucl. Phys. **31**, 607 (1980)].

[82]V. G. Soloviev, in: Proceedings of the International Conference on the Interactions of Neutrons with Nuclei, Vol. 1, Lowell, 1976, p. 421.

[83]V. E. Bunakov and S. G. Ogloblin, Preprint No. 319, Leningrad Institute of Nuclear Physics, Leningrad, 1977.

[84]F. L. Shapiro, Research Applications of Nuclear Pulsed Systems, IAEA, Vienna, 1967, p. 176.

[85]V. P. Alfimenkov *et al.*, Yad. Fiz. **17**, 13 (1973) [Sov. J. Nucl. Phys. **17**, 6 (1973)].

[86]V. P. Alfimenkov *et al.*, Nucl. Phys. **A267**, 172 (1976).

[87]R. N. Kuklin, Yad Fiz. **6**, 969 (1967) [Sov. J. Nucl. Phys. **6**, 706 (1968)].

[88]G. G. Bunatyan, Preprint R4-8889, Joint Institute for Nuclear Research, Dubna, 1975.

[89]G. G. Bunatyan, Yad. Fiz. **26**, 44 (1977) [Sov. J. Nucl. Phys. **26**, 22 (1977)].

[90]A. I. Blokhin and A. V. Ignatyuk, Cited in Ref. 43, Part 3, p. 13.

[91]V. V. Voronov and V. G. Solov'ev, Yad. Fiz. **16**, 1188 (1972) [Sov. J. Nucl. Phys. **16**, 653 (1973)].

[92]V. K. Ignatovich, Yu. M. Ostanevich and L. Cher, Preprint R4-7296, Joint Institute for Nuclear Research, Dubna, 1973.

[93]W. E. Lamb, Phys. Rev. **55**, 190 (1939).

[94]K. Zaidel' *et al.*, Dokl. Akad. Nauk SSSR **256**, 360 (1981) [Sov. Phys. Dokl. **26**, 54 (1981)].

[95]A. Meister *et al.*, Nucl. Phys. **A362**, 18 (1981).

[96]G. K. Shenoy and F. E. Wagner (editors), Mössbauer Isomer Shifts, North-Holland, Amsterdam, 1978.

[97]S. A. De Wit *et al.*, Nucl. Phys. **87**, 657 (1967).

[98]G. G. Bunatyan, Yad. Fiz. **26**, 979 (1977) [Sov. J. Nucl. Phys. **26**, 518 (1977)]; **29**, 10 (1979) [Sov. J. Nucl. Phys. **29**, 4 (1979)].

[99]L. D. Landau and Ya. A. Smorodinskii, Zh. Eksp. Teor. Fiz. 14, 269 (1944); Ya. A. Smorodinskii, Zh. Eksp. Teor. Fiz. 15, 89 (1945).

[100]H. A. Bethe and P. Morrison, Elementary Nuclear Theory, Wiley, New York, 1956 (Russ. transl. IL, Moscow, 1958).

[101]G. L. Squirs and A. I. Stewart, Proc. R. Soc. **A230**, 19 (1955).

[102]L. Koester and W. Nistler, Z. Phys. **272**, 189 (1975); W. Dilg, Phys. Rev. **C11**, 103 (1975).

[103]W. Dilg, L. Koester, and W. Nistler, Phys. Lett. **B36**, 208 (1971).

[104]V. P. Alfimenkov *et al.*, Phys. Lett. **B24**, 151 (1967).

[105]H. P. Nagels *et al.*, Nucl. Phys. **B147**, 189 (1979).

[106]V. N. Efimov, in: Mezhdunarodnyi simpozium po probleme neskol'kikh tel (International Symposium on the Many-Body Problem), D4-12366, OIYaI, Dubna, 1979, pp. 59, 61.

[107]V. F. Kharchenko, in: Trudy Mezhdunarodnogo simpoziuma po probleme neskol'kikh tel v yadernoi fizike (Proceedings of the International Symposium on the Many-Body Problem in Nuclear Physics), D4-80-271, OIYaI, Dubna, 1980, p. 9; Fiz. Elem. Chastits At. Yadra. 10, 884 (1979) [Sov. J. Part. Nucl. **10**, 349 (1979)].

[108]V. P. Alfimenkov *et al.*, Yad. Fiz. 25, 1145 (1977) [Sov. J. Nucl. Phys. **25**, 607 (1977)]; É. I. Sharapov, in: III Mezhdunarodnaya shkola po neitronnoi fizike (Third International School on Neutron Physics), D3-11787, OIYaI, Dubna, 1978, p. 437.

[108]H. Kaiser *et al.*, Z. Phys. **A291**, 231 (1979).

[110]V. P. Alfimenkov *et al.*, Yad. Fiz. **33**, 891 (1981) [Sov. J. Nucl. Phys. **33**, 467 (1981)].

[111]T. W. Phillips, B. L. Berman, and J. D. Seagrave, Phys. Rev. **C22**, 384 (1980); Phys. Lett. **B91**, 200 (1980).

[112]E. Feenberg, Phys. Rev. **49**, 328 (1936).

[113]A. A. Bergman *et al.*, in: Yadernye reaktsii pri malykh i srednikh énergiyakh (Nuclear Reactions at Low and Intermediate Energies), Izd. AN SSSR, Moscow, 1957, p. 17; Zh. Eksp. Teor. Fiz. 33, 9 (1957) [Sov. Phys. JETP **6**, 6 (1957)].

[114]L. Passel and R. I. Schermer, Phys. Rev. 150, 146 (1966).

[115]S. B. Borzakov *et al.*, Yad. Fiz. 35, 532 (1982) [Sov. J. Nucl. Phys. **35**, 307 (1982)].

[116]M. Baumgartner *et al.*, Nucl. Phys. **A368**, 189 (1981).

[117]J. J. Bevelacque, Can. J. Phys. **57**, 1833 (1979).

[118]V. A. Vesna *et al.*, Nucl. Phys. **A352**, 181 (1981).

[119]É. I. Sharapov, Fiz. Elem. Chastits At. Yadra. 12, 962 (1981) [Sov. J. Part. Nucl. **12**, 386 (1981)].

[120]V. P. Alfimenkov *et al.*, Yad. Fiz. 32, 1491 (1980) [Sov. J. Nucl. Phys. **32**, 771 (1980)].

[121]D. O. Riska and G. E. Brown, Phys. Lett. **B38**, 193 (1972).

[122]E. Hadjimichael, Phys. Rev. Lett. 31, 183 (1973).

[123]V. P. Alfimenkov *et al.*, Yad. Fiz. 31, 21 (1980) [Sov. J. Nucl. Phys. **31**, 10 (1980)].

[124]M. Suffert and R. Berthollet, Nucl. Phys. **A318**, 54 (1979).

[125]I. S. Towner and F. C. Khanna, Nucl. Phys. **A356**, 445 (1979).

[126]V. N. Andreev, in: II Mezhdunarodnaya shkola po neitronnoi fizike (Second International School on Neutron Physics), D3-7991, OIYaI, Dubna, 1974, p. 96.

Translated by Dave Parsons

322   Sov. Phys. Usp. 25(5), May 1982

Pikel'ner *et al.*   322